REVIEW ARTICLES

Giant Multiporphyrin Arrays as Artificial Light-Harvesting Antennas

Hiroshi Imahori*

Department of Molecular Engineering, Graduate School of Engineering, Kyoto University, PRESTO, Japan Science and Technology Agency (JST), Katsura, Nishikyo-ku, Kyoto 615-8510 (Japan), and Fukui Institute for Fundamental Chemistry, Kyoto University, 34-4, Takano-Nishihiraki-cho, Sakyo-ku, Kyoto 606-8103, Japan

Received: December 30, 2003

Synthetic giant multiporphyrin arrays with well-defined architectures are reviewed in terms of artificial light-harvesting materials. Meso,meso-linked porphyrin arrays and multiporphyrin dendrimers have successfully mimicked the light-harvesting function of bacterial photosynthetic systems. We have also developed novel multiporphyrin-modified metal nanoclusters where porphyrins employed as a light-harvesting unit are well organized onto metal nanoclusters by self-assembly processes. Multiporphyrin-modified metal nanoclusters have been applied to photocatalyses and photovoltaic cells. In particular, they have been assembled with fullerenes step-by-step to make large, uniform clusters on nanostructured semiconductor electrodes, which exhibit a high power-conversion efficiency close to 1%. These systems provide valuable information on the design of porphyrin molecular assemblies that can be tailored to construct molecular photonic devices as well as artificial photosynthetic systems.

1. Introduction

Recently, many studies have been focused on using artificial photosynthesis to develop light-energy conversion systems as well as molecular photonic devices.[1−4] The natural photosynthetic system is regarded as one of the most elaborate nanobiological machines.[5] It converts solar energy into an electrochemical potential or chemical energy, which is a prerequisite for the living organisms on the earth. The core function of photosynthesis is a cascade of photoinduced energy and electron transfer between donors and acceptors in the antenna complexes and the reaction center. For instance, in purple photosynthetic bacteria (*Rhodopseudomonas acidophila* and *Rhodopseudomonas palustris*), there are two different types of antenna complexes: a core light-harvesting antenna (LH1) and a peripheral light-harvesting antenna (LH2).[6] LH1 surrounds the reaction center where charge separation occurs. Peripheral antenna LH2 forms two wheel-like structures: B800 with 9 bacteriochlorophyll *a* (Bchl *a*) molecules and B850 with 18 Bchl *a* molecules, which are noncovalently bound to two types of transmembrane helical α and β apoproteins. Carotenoids near the chlorophylls absorb sunlight in the spectral region where chlorophyll molecules absorb weakly and transfer the resultant excitation energy to the chlorophyll molecules via singlet−singlet energy transfer. The collected energy then transfers from LH2 to LH1, in which the excitation energy migrates to the wheel-like arrays of chlorophylls of LH1 and LH2 and in turn is funneled into the chlorophyll dimer (special pair) in the reaction center.[6] A unidirectional electron-transfer event takes place along the array of chromophores embedded in the transmembrane protein in a sequence of special pairs−accessory chlorophyll, pheophytin, quinone A, and quinone B−producing a long-lived, charge-separated state across the membrane with a quantum efficiency of nearly 100%.[7] The resultant charge-separated state ultimately leads to the production of adenosine triphosphate (ATP) via the proton gradient generated across the membrane.[1]

Light-harvesting systems also show great variety in their structures. For instance, in purple bacteria, more than nine chlorophylls are organized in symmetric ringlike structures (vide supra),[6] whereas in green bacteria, a large number of chlorophylls are arranged into rodlike aggregates without the help of proteins.[8] In contrast, chlorophyll aggregates in photosystem (PS) I of cyanobacteria and higher plants exhibits a rather random array forming 2D structures, which surround the reaction center.[9,10] Such complex structure and diversity in natural light-harvesting systems have made it difficult to understand the unique relationship between structure and function in the light-harvesting systems. In this context, synthetic multiporphyrin arrays have been frequently prepared to shed light on the light-harvesting processes[11−17] because (i) porphyrins are more stable and accessible synthetically than chlorophylls and (ii) their absorption properties are similar in that they absorb strongly in the blue and weakly or moderately in the green regions. However, no synthetic method had allowed organic chemists to prepare giant covalent or noncovalent arrays of porphyrins (10 or more) with well-defined geometries. During the past decade, the challenge of creating such artificial light-harvesting systems has prompted the development of novel synthetic ways to produce a diverse collection of giant multiporphyrin arrays.[18−26] There are two different methodologies for preparing well-defined architectures comprising more than 10 porphyrin units. Examples of covalent bonding methodology include (i) linear arrays with direct meso,meso linkages[18] and (ii) dendritic arrays with a variety of linkers,[19−21] whereas those of noncovalent bonding (self-assembly) methodology involve (iii) planar or

* E-mail: imahori@scl.kyoto-u.ac.jp.

10.1021/jp038036b CCC: $27.50
Published on Web 04/27/2004

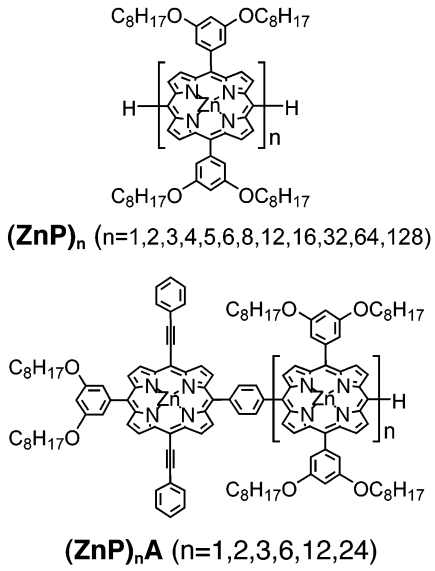

Figure 1. Meso,meso-linked multiporphyrin arrays $(ZnP)_n$ ($n = 1-6$, 8, 12, 16, 32, 64, 128) and $(ZnP)_nA$ ($n = 1-3$, 6, 12, 24).

spherical arrays on metal or semiconductor surfaces using self-assembly,[22−24] (iv) cyclic arrays with hydrogen or coordination bonding,[25] and (v) sheetlike arrays with metal-coordinated pyridyl linkages.[26]

In this review, we highlight the structure and photophysical properties of the giant multiporphyrin arrays (more than 10 porphyrins) including meso,meso-linked porphyrins, multiporphyrin dendrimers, and multiporphyrin-modified metal nanoclusters. The structures and photophysical properties of the three systems together with natural systems are compared to obtain a better understanding of the light-harvesting processes. In particular, multiporphyrin-modified metal nanoclusters are shown to be highly promising building blocks for photocatalysis and organic solar cells throughout our studies.

2. Giant Multiporphyrin Arrays

2.1. Meso,meso-Linked Multiporphyrin Arrays. Recently, there has been a remarkable advance in the synthesizing capabilities of long rodlike porphyrin arrays in which porphyrin chromophores are directly connected together through meso positions up to 128 units ($(ZnP)_n$, $n = 1-6$, 8, 12, 16, 32, 64, 128) (Figure 1).[27] The alternating orthogonal conformation between the adjacent porphyrin units in the meso,meso-linked porphyrin arrays minimizes electronic communication over the array despite the extremely short interporphyrin distance of 8.4 Å. The large absorption cross section and the wide absorption profile (300−700 nm) in the giant porphyrin arrays are highly suitable as light-harvesting model systems. The coherent length in strongly coupled molecular arrays is known to reflect the collective behavior of the transition dipole moments of chromophores aligned within the arrays.[27] The coherent length in the excited singlet state of $(ZnP)_n$ is estimated to be 4 to 5, which is virtually the same as the value of the strongly coupled B850 ring in LH2.[27] Energy-transfer processes have also been investigated in energy donor−acceptor systems in which a meso,meso-bisphenylethynylated porphyrin acceptor (A) is linked via a 1,4-phenylene spacer at the end meso position of energy-donating $(ZnP)_n$ ($(ZnP)_nA$, $n = 1-3$, 6, 12, 24) (Figure 1).[28] Efficient energy transfer was observed for $(ZnP)_nA$ with time constants of 4.0×10^{11} s^{-1} [$(ZnP)_1A$], 3.0×10^{11} s^{-1} [$(ZnP)_2A$], 1.8×10^{11} s^{-1} [$(ZnP)_3A$], 4.8×10^{10} s^{-1} [$(ZnP)_6A$], 1.6×10^{10} s^{-1} [$(ZnP)_{12}A$], and 9.3×10^{9} s^{-1} [$(ZnP)_{24}A$] in toluene, although the energy-transfer efficiency of the longest porphyrin rod $(ZnP)_{24}A$ is not quantitative because of the unequal distribution in the exciton location or the conformational heterogeneity.[28] These results have been well rationalized by a revised Förster equation, which takes into account an exciton extending coherently over several porphyrin chromophores in $(ZnP)_n$.[28] Overall, meso,meso-linked porphyrin arrays are promising in light of mimicking natural light-harvesting arrays, owing to the fast energy migration as well as enhanced light-collecting properties in the visible region.

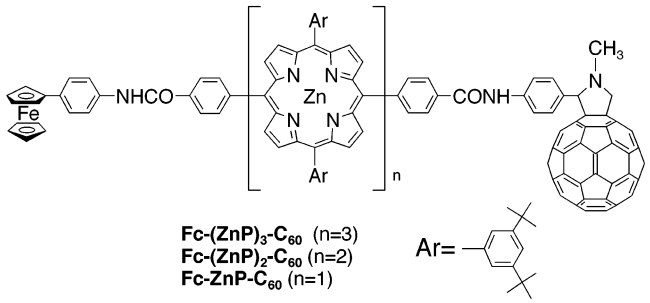

Figure 2. Ferrocene−porphyrin−C_{60} triad (Fc−ZnP−C_{60}), ferrocene-meso,meso-linked porphyrin dimer−C_{60} tetrad (Fc−$(ZnP)_2$−C_{60}), and ferrocene-meso,meso-linked porphyrin trimer−C_{60} pentad (Fc−$(ZnP)_3$−C_{60}).

Because meso,meso-linked porphyrins are excellent light-harvesting antennas, meso-,meso-linked porphyrin oligomers have been combined with charge-separation molecules to mimic both the light-harvesting and charge-separation functions.[29−31] For instance, meso-,meso-linked porphyrin dimer $(ZnP)_2$ and trimer $(ZnP)_3$ as light-harvesting chromophores were incorporated into photosynthetic multistep electron-transfer models including ferrocene (Fc) as an electron donor and fullerene (C_{60}) as an electron acceptor to construct ferrocene-meso,meso-linked porphyrin dimer−fullerene tetrad Fc−$(ZnP)_2$−C_{60} [31b] and ferrocene-meso,meso-linked porphyrin trimer−fullerene pentad Fc−$(ZnP)_3$−C_{60} [31c] (Figure 2). The photoirradiation of Fc−$(ZnP)_2$−C_{60} in polar solvents results in photoinduced electron transfer from the excited singlet state of porphyrin dimer $^1(ZnP)_2$* to the C_{60} moiety to produce the porphyrin dimer radical cation−C_{60} radical anion pair, Fc−$(ZnP)_2^{\bullet+}$−$C_{60}^{\bullet-}$. In competition with the back electron transfer from $C_{60}^{\bullet-}$ to $(ZnP)_2^{\bullet+}$ to regenerate the ground state, an electron transfer from Fc to $(ZnP)_2^{\bullet+}$ occurs to give the final charge-separated state, Fc^+-$(ZnP)_2$−$C_{60}^{\bullet-}$ (R_{ee} = 38.6 Å), which is detected as the transient absorption spectra by laser flash photolysis. The quantum yield of formation of the final charge-separated state was determined to be 0.88 in benzonitrile.[31b] The final charge-separated state decayed, obeying first-order kinetics with a lifetime of 19 μs in benzonitrile at 295 K. The activation energy for the charge-recombination process was determined to be 0.15 eV in benzonitrile, which is much larger than the value expected from the direct charge-recombination process to the ground state. This value is comparable to the energy difference between the intermediate charge-separated state (Fc−$(ZnP)_2^{\bullet+}$−$C_{60}^{\bullet-}$) and the final charge-separated state (Fc^+-$(ZnP)_2$−$C_{60}^{\bullet-}$). This indicates that back electron transfer to the ground state occurs via the reverse stepwise processes—a rate-limiting electron transfer from $(ZnP)_2$ to Fc^+ to give the intermediate charge-separated state (Fc−$(ZnP)_2^{\bullet+}$−$C_{60}^{\bullet-}$) followed by a fast electron transfer from $C_{60}^{\bullet-}$ to $(ZnP)_2^{\bullet+}$ to regenerate the ground state, Fc−$(ZnP)_2$−C_{60}.[31b] This is in sharp contrast to the extremely slow direct charge-recombination process of the bacteriochlorophyll dimer radical cation−quinone radical anion pair in bacterial reaction centers.[1] A high quantum yield results from

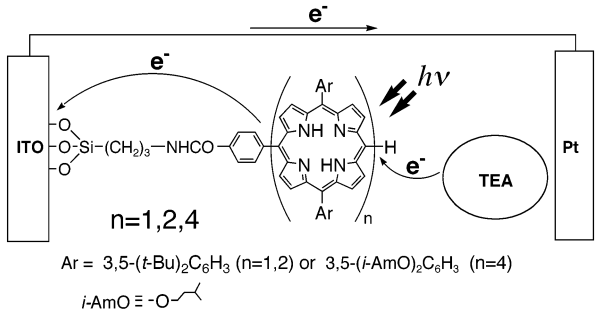

Figure 3. Photoinduced electron transfer at ITO electrodes modified with self-assembled monolayers of meso,meso-linked porphyrin oligomers (n = 1, 2, 4).

the efficient charge separation through the porphyrin dimer, and the fast charge recombination is associated with the delocalized porphyrin radical cation in the porphyrin dimer.[32]

The photoexcitation of Fc−$(ZnP)_3$−C_{60} in polar solvents leads to the formation of Fc^+-$(ZnP)_3$−$C_{60}^{\bullet-}$, as in the case of Fc−$(ZnP)_2$−C_{60}.[31c] In contrast to Fc−$(ZnP)_2$−C_{60}, the decay dynamics of the final charge-separated radical ion pair [Fc^+-$(ZnP)_3$−$C_{60}^{\bullet-}$] obeyed second-order kinetics with a second-order rate constant of 2.7×10^9 M^{-1} s^{-1}, which is nearly diffusion-controlled. The preference of such an intermolecular ET (second-order kinetics) over an intramolecular ET (first-order kinetics) indicates that the intramolecular charge recombination from the $C_{60}^{\bullet-}$ to the Fc^+ moiety is too slow to compete with the intermolecular ET. The final charge-separated state in frozen DMF at 163 K decays, obeying first-order kinetics with a lifetime of 0.53 s as a result of the suppression of diffusional intermolecular ET. Such a long lifetime of the charge-separated state is comparable with that of the natural bacterial photosynthetic reaction center. More importantly, the quantum yield of formation of the final charge-separated state (0.83 in benzonitrile) remains high despite the large separation distance between the Fc^+ and $C_{60}^{\bullet-}$ moieties (R_{ee} = 46.9 Å). The efficient charge separation through the porphyrin trimer is responsible for the high quantum yield, whereas extremely slow charge recombination is associated with the localized porphyrin radical cation in the middle porphyrin of the porphyrin trimer, which is in sharp contrast to that of the delocalized porphyrin radical cation in the porphyrin dimer.[32] The light-harvesting efficiency in the visible region has also been much improved in Fc−$(ZnP)_3$−C_{60} as compared to that of Fc−ZnP−C_{60} [31a] because of exciton coupling in the porphyrin trimer as well as an increase in the number of porphyrins.[31a,b]

Meso,meso-linked porphyrin oligomers have also been applied to molecular photovoltaic devices. A systematic series of ITO electrodes modified covalently with self-assembled monolayers of meso,meso-linked porphyrin oligomers have been designed to provide valuable insight into the development of artificial photosynthetic devices (Figure 3).[32] Photoelectrochemical measurements were performed in an argon-saturated 0.1 M Na_2SO_4 aqueous solution containing triethanolamine (TEA) as a sacrificial electron donor or methyl viologen (MV^{2+}) as an electron acceptor in a three-electrode system including the modified ITO electrodes. The action spectrum of the porphyrin oligomer systems exhibits photocurrent generation in a wide wavelength region, demonstrating the enhancement of light-harvesting properties in the visible region. The relative integrated value of the action spectrum and the internal quantum yield of photocurrent generation of the self-assembled monolayers of the porphyrin oligomer increase with an increasing number of porphyrins.[32]

These results clearly demonstrate that meso,meso-linked porphyrin arrays are highly promising as building blocks of both molecular photovoltaic devices and photosynthetic models including artificial light-harvesting units.

2.2. Multiporphyrin Dendrimers. Dendrimers are well-defined, hyperbranched, 3D macromolecules with a regular treelike array of branch units.[33] Such unique morphology has revealed potential applications in the field of host−guest chemistry, analytical chemistry, catalysis, molecular electronics, biology, medicine, and artificial photosynthesis. In particular, dendrimeric architectures have attracted increasing attention as artificial light-harvesting systems in terms of their structural analogy to natural antenna complexes. Along this line, multiporphyrin dendrimers with well-defined geometries have rapidly appeared.[19−21]

Porphyrin-based dendrimeric arrays can be prepared in either a convergent or divergent manner. Convergent synthesis employing porphyrin building blocks has afforded multiporphyrin arrays $(ZnP)_nH_2P$ containing zinc porphyrins (n = 1, 2, 8, 20) and one free base porphyrin joined via diarylethyne linkers (Figure 4).[19b] The yields and ease of purification are unsatisfactory when the number of porphyrins is large. Efficient singlet−singlet energy migration occurs among the $(ZnP)_n$, followed by energy transfer to the H_2P in each of the arrays, with the overall time constant of the process decreasing monotonically with an increasing number (n) of $(ZnP)_n$ molecules (n = 1 (2.2×10^{10} s^{-1}), 2 (1.1×10^{10} s^{-1}), 8 (9.5×10^9 s^{-1}), and 20 (4.5×10^9 s^{-1}) in toluene), together with the overall energy-transfer efficiencies decreasing slightly with an increasing number (n) of $(ZnP)_n$ molecules (n = 1 (98%), 2 (96%), 8 (96%), and 20 (92%) in toluene).[19b]

The generation number and morphology effects on intramolecular energy transfer in a series of star- and cone-shaped dendritic multiporphyrin arrays $(nZnP)_4H_2P$ and $(nZnP)_1H_2P$, n = 1, 3, 7) have been investigated by picosecond time-resolved fluorescence spectroscopy and steady-state fluorescence depolarization measurements (Figure 5).[20] For the star-shaped series [$(nZnP)_4H_2P$], the energy-transfer efficiency from the excited singlet state of $(nZnP)_4$ to the core H_2P decreases significantly with an increase in the generation number (87% (n = 1), 80% (n = 3), 71% (n = 7) in THF). Such a trend is remarkably evident for the cone-shaped series [$(nZnP)_1H_2P$]; the energy-transfer efficiency from the excited singlet state of $(nZnP)_1$ to the core H_2P decreases dramatically with an increase in the generation number (86% (n = 1), 66% (n = 3), 19% (n = 7) in THF). Fluorescence depolarization studies in poly(ethylene glycol) containing THF reveal the low polarization values for star-shaped $(7ZnP)_4H_2P$ (0.03) and $(3ZnP)_4H_2P$ (0.05) relative to those for cone-shaped $(7ZnP)_1H_2P$ (0.10) and $(3ZnP)_1H_2P$ (0.11), respectively, indicating an efficient energy migration among the zinc porphyrin units in the star-shaped series relative to that in the cone-shaped series. These contrasting trends suggest a possible cooperation of the four dendritic zinc porphyrin wedges in the large $(7ZnP)_4H_2P$ molecule, thus facilitating energy migration and energy transfer among the porphyrins, as seen in the light-harvesting processes of photosynthesis.[20]

The coupling of porphyrin-activated ester with appropriate first-, second-, third-, fifth-generation polypropylenimine dendrimers has given multiporphyrin arrays (DnH_2Pn), where n (n = 4, 8, 16, 64) is the number of porphyrin end-groups (Figure 6).[21b] The porphyrins are assumed to be randomly arranged on the surface of a sphere for the dendrimers. A depolarization of the fluorescence in $D4H_2P4$, $D16H_2P16$, and $D64H_2P64$ as

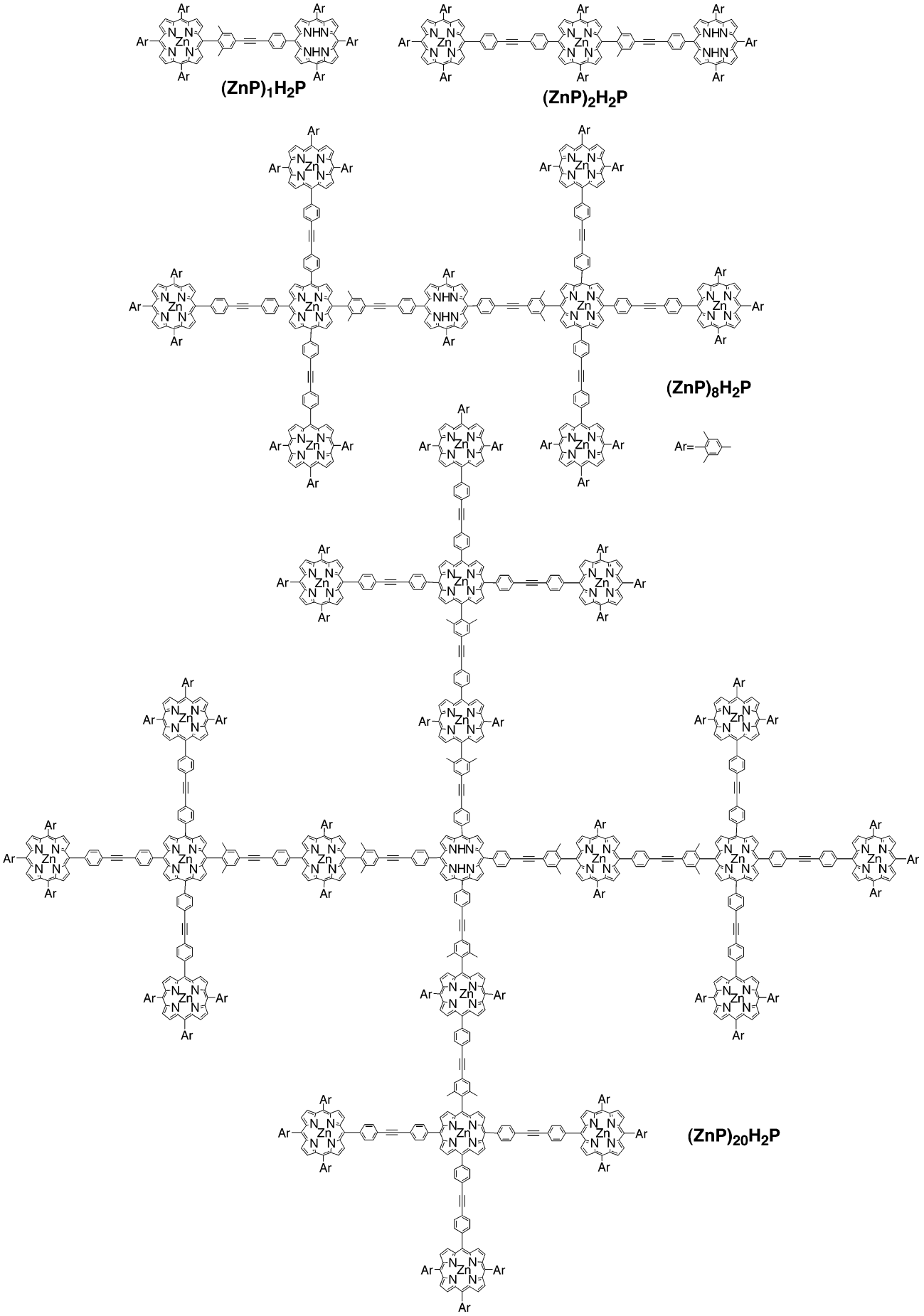

Figure 4. Porphyrin dimer [$(ZnP)_1H_2P$], trimer [$(ZnP)_2H_2P$], nonamer [$(ZnP)_8H_2P$], and 21mer [$(ZnP)_{20}H_2P$].

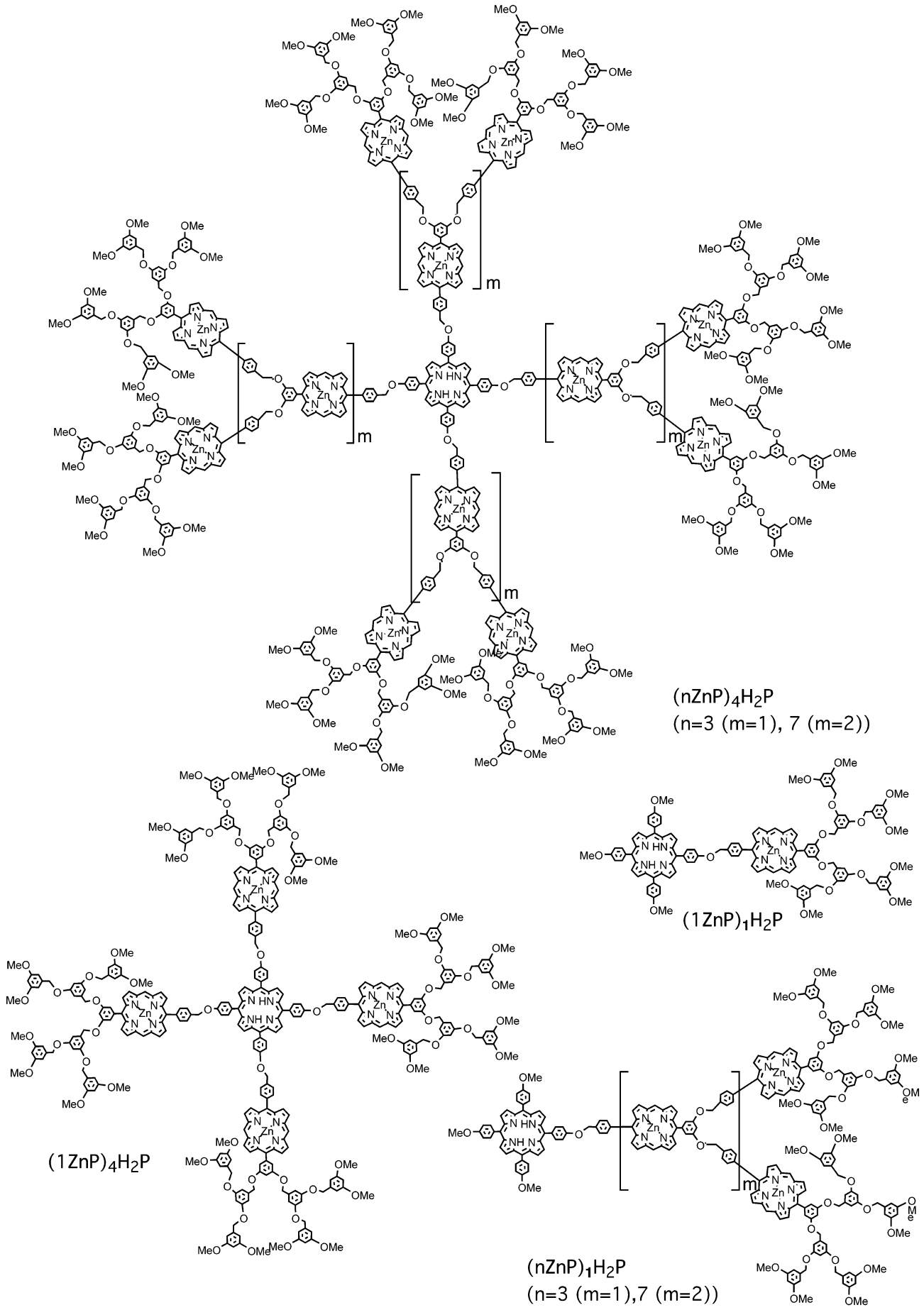

Figure 5. Porphyrin dendrimers $(n\text{ZnP})_4\text{H}_2\text{P}$ (n = 1, 3, 7) and $(n\text{ZnP})_1\text{H}_2\text{P}$ (n = 1, 3, 7).

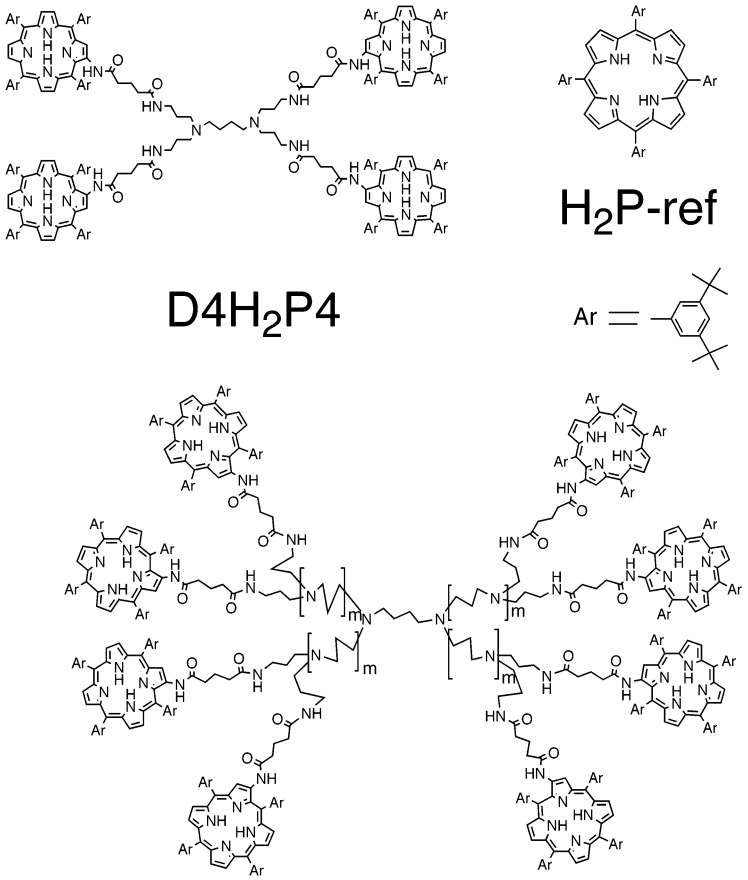

Figure 6. Porphyrin dendrimers D4H_2P4, D8H_2P8, D16H_2P16, and D64H_2P64 and reference H_2P-ref.

compared to that of the porphyrin monomer reference (H_2P-ref) suggests that energy migration takes place between the chromophores within the dendrimer. In particular, the fluorescence depolarization of D64H_2P64 is explained rationally by a model that includes independent and simultaneously rapid energy migration between porphyrins contained on the surface of the dendrimer sphere and slow energy migration between porphyrins in irregular dendrons most like found either outside or inside the sphere.[21b]

Recently, high-efficiency organic photovoltaic devices have attracted much attention in terms of low cost, flexibility, and ubiquitousness.[34−37] They include two types of organic solar cells: dye-sensitized [34] and bulk heterojunction.[36,37] In dye-sensitized solar cells, ultrafast photoinduced charge separation and retarded charge recombination take place at the interface between the dye and the nanocrystalline semiconductor (i.e., TiO_2), which has a remarkably large surface area, to improve the light-harvesting efficiency relative to that of the monolayer system.[34] Namely, the excited dye injects an electron into the conduction band of the semiconductor, and the oxidized dye is reduced by an electron donor (I^-) in the electrolyte. The electron flows through the external circuit to reduce the oxidized donor (I_3^-), resulting in the recovery of the initial state. The maximum overall efficiencies that have been reported are in the 7−11% range.[34] In bulk heterojunction solar cells, photoinduced charge separation occurs at the blend interface between the donor (i.e., conjugated polymers) and acceptor (i.e., fullerenes or conjugated polymers), where interpenetrating, bicontinuous phase-segregated layers are formed.[36,37] By mixing the donor and the acceptor on an intimate scale, the interface is distributed throughout the mixed film. Thus, all photogenerated excitons can be separated easily before recombination. For instance, in the case of the polymer−fullerene device, the photoinduced charge separation is extremely fast (within 0.1 ps) with a quantum efficiency close to unity, and the charge-separated state is unusually stable (up to milliseconds of the lifetime at 80 K)[37] owing to the small reorganization energies of fullerenes (vide infra).[4,38] A recently reported polymer−fullerene device reached a power-conversion efficiency of up to 3.0−3.5%.[37] However, more importantly, the electrons and holes should also travel through the respective "electron-and-hole highway" in the blend film to avoid charge recombination. Such a nanostructured electron-and-hole highway has been suggested to be crucial to improving the performance of organic solar cells.[37]

Porphyrins (electron donor) are known to be spontaneously attracted to fullerenes (electron acceptor).[39] In addition, a combination of porphyrins and fullerenes has been found to be useful for generating a long-lived charge-separated state with a high quantum yield.[4,31,38,40] Thus, multiporphyrin dendrimers are expected to sandwich fullerenes between the porphyrins in the supramolecular complex. Such supramolecular architecture seems ideal for fulfilling the enhanced light-harvesting efficiency of chromophores throughout the solar spectrum and the highly efficient conversion of the harvested light into the high-energy state of the charge separation by photoinduced electron transfer. Recently, we have successfully constructed the novel light-energy conversion system using supramolecular complexes of multiporphyrin dendrimers with fullerenes by clusterization in

a mixed solvent on nanostructured SnO_2 electrodes.[41] Successive molecular assembly makes it possible to control the 3D architecture, which is essential for light-energy conversion.

Porphyrin dendrimers (primary organization, D*n*H_2P*n* (Figure 6)) form supramolecular complexes with fullerene molecules in toluene (secondary organization), and they cluster in an acetonitrile/toluene mixed-solvent system (ternary organization).[42,43] Then, the clusters are deposited on nanostructured SnO_2 electrodes by an electrophoretic deposition method according to Kamat's method (quaternary organization, Figure 11).[42,43] The electronic absorption spectra of (D*n*H_2P*n* + C_{60})$_m$ and (H_2P-ref + C_{60})$_m$ in a 3:1 acetonitrile/toluene mixture are much broader than those in toluene, indicating the formation of clusters in the mixed solvent.[41] The broad, long-wavelength absorption (500−800 nm) is diagnostic of the charge-transfer absorption band due to the π complex formed between the porphyrin and C_{60}.[39b,c]

The TEM image of (D8H_2P8 + C_{60})$_m$ shows large nanoclusters of 200−300 nm diameter with a well-controlled size and shape. This is in sharp contrast to the clusters of (H_2P-ref + C_{60})$_m$, which are irregular and small. These results clearly show that dendritic structure plays an important role in controlling the formation of molecular clusters. Judging from the TEM data, we can conclude that D*n*H_2P*n* molecules are self-assembled with C_{60} molecules in the mixed solution to yield large donor−acceptor (D−A) nanoclusters with an interpenetrating network.[41]

Upon subjecting the resultant cluster suspension to a high electric dc field, mixed D*n*H_2P*n* and C_{60} clusters [(D*n*H_2P*n* + C_{60})$_m$] and reference clusters [(H_2P-ref + C_{60})$_m$] were deposited onto an ITO electrode covered with SnO_2 nanoparticles (ITO/SnO_2) to give modified electrodes (denoted as ITO/SnO_2/(D*n*H_2P*n* + C_{60})$_m$ (n = 4, 8, 16) and ITO/SnO_2/(H_2P-ref + C_{60})$_m$), respectively. The absorptivity of the ITO/SnO_2/(D*n*H_2P*n* + C_{60})$_m$ system is much enhanced compared with that of the system with clusters made from the porphyrin reference. These results ensure that incident light is collected intensively in the visible and near-infrared regions by ITO/SnO_2/(D*n*H_2P*n* + C_{60})$_m$.[41] The AFM image of ITO/SnO_2/(D4H_2P4 + C_{60})$_m$ reveals cluster aggregation with a regular size of 50−100 nm, which is consistent with the TEM data.[41]

Photoelectrochemical measurements were performed with a standard two-electrode system consisting of the modified ITO working electrode and a Pt wire gauze electrode in 0.5 M NaI and 0.01 M I_2 in air-saturated acetonitrile. First, we examined the concentration effect of C_{60} on the photoelectrochemical properties of the ITO/SnO_2/(D*n*H_2P*n* + C_{60})$_m$/NaI + I_2/Pt device. The IPCE values increase with increasing C_{60} concentration (0−0.31 mM in acetonitrile/toluene) at constant concentration based on the porphyrin moieties (0.19 mM). This indicates that electron transfer from the excited singlet state of the porphyrin to C_{60} takes place, leading to efficient photocurrent generation.[41]

IPCE values of ITO/SnO_2/(D*n*H_2P*n* + C_{60})$_m$/NaI + I_2/Pt devices (n = 4, 8) exhibit a remarkable increase as compared with those of the reference device (ITO/SnO_2/(H_2P-ref + C_{60})$_m$/NaI + I_2/Pt). In particular, the ITO/SnO_2/(D4H_2P4 + C_{60})$_m$/NaI + I_2/Pt device has a maximum IPCE value of 15% as well as an enhanced photoelectrochemical response in the UV−vis and near-IR regions (400−1000 nm). Such an effective photoenergy conversion is largely ascribed to the dendritic structure to control the 3D organization between the porphyrin and C_{60} in the mixed thin films on the nanostructured SnO_2 electrode. It should be noted here that the IPCE value of the ITO/SnO_2/(D16H_2P16 + C_{60})$_m$/NaI + I_2/Pt device becomes smaller than

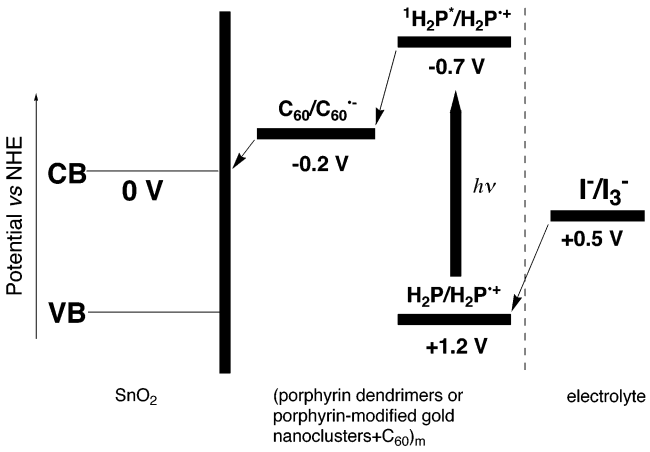

Figure 7. Energy-level diagram of light-energy conversion system using supramolecular complexes of porphyrin dendrimers or multiporphyrin-modified gold nanoclusters with fullerene by clusterization in mixed solvent on nanostructured SnO_2 electrodes.

the value of the reference device irrespective of the high generation. This may be caused by the steric effect of porphyrin moieties of dendrimers in the higher generation, which inhibits the $\pi-\pi$ interaction with C_{60}.[41]

The ITO/SnO_2/(D4H_2P4 + C_{60})$_m$/NaI + I_2/Pt device has a much larger fill factor (FF) of 0.31, open circuit voltage (V_{OC}) of 220 mV, short circuit current density (I_{SC}) of 0.29 mA cm^{-2}, and overall power conversion efficiency (η) of 0.32% at an input power (W_{IN}) of 6.2 mW cm^{-2}. The η value of ITO/SnO_2/(D4H_2-P4 + C_{60})$_m$/NaI + I_2/Pt device is 10 times as large as that of the ITO/SnO_2/(H_2P-ref + C_{60})$_m$/NaI + I_2/Pt device (η = 0.035%) under the same experimental conditions.[41]

Photocurrent generation in the present device is initiated by photoinduced charge separation from the porphyrin excited singlet state ($^1H_2P^*/H_2P^{\bullet+}$ = −0.7 V vs NHE)[43] in the dendrimer to C_{60} ($C_{60}/C_{60}^{\bullet-}$ = −0.2 V vs NHE)[43] in the porphyrin dendrimer−C_{60} complex rather than by direct electron injection into the conduction band of the SnO_2 (0 V vs NHE)[43] system, as illustrated in Figure 7. The reduced C_{60} injects electrons into the SnO_2 nanocrystallites, whereas the oxidized porphyrin ($H_2P/H_2P^{\bullet+}$ = 1.2 V vs NHE)[43] undergoes an electron-transfer reduction with the iodide (I^-/I_3^- 0.5 V vs NHE)[43] in the electrolyte system.[41]

This device exhibits an efficient photoelectrochemical response in visible and near-IR regions and high power-conversion efficiency as compared with that of the reference device because of ultrafast, efficient electron transfer from the porphyrin excited singlet state to fullerene within the dendritic matrix in which the porphyrin and fullerene moieties are in close proximity. Unfortunately, however, the higher generation of such dendritic structures does not allow the porphyrin to make intimate contact with the fullerene, reducing the performance of the solar cell, which is in sharp contrast to the behavior of the supramolecular solar cell comprising multiporphyrin-modified gold nanoclusters and fullerenes on nanostructured SnO_2 electrode, where fullerene molecules are well incorporated between the porphyrins (vide infra).

2.3. Multiporphyrin-Modified Metal Nanoclusters. Covalently linked multiporphyrin arrays bearing more than 10 porphyrin units are found to be superior to the corresponding porphyrin monomers and oligomers with respect to structural control and light-harvesting properties, but the synthetic difficulty makes it difficult to employ such covalently linked multiporphyrin arrays in terms of practical applications. Another

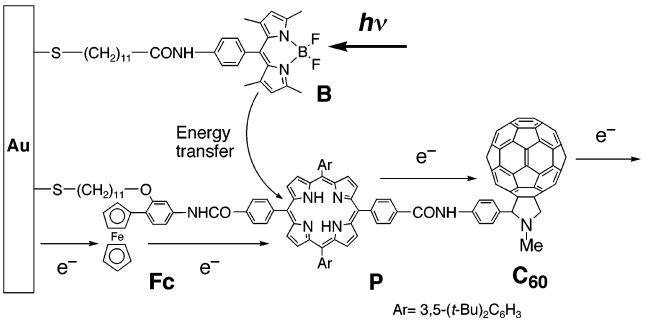

Figure 8. Photoinduced energy and electron transfer at gold electrodes modified with mixed self-assembled monolayers of the boron dipyrrin (B) dye (light-harvesting molecule) and the ferrocene (Fc)−porphyrin (P)−fullerene (C_{60}) triad (charge-separation molecule).

promising approach for achieving these goals is the self-assembly of porphyrin-bearing molecular recognition units. These porphyrin self-assemblies are prepared easily but often afford less complete structural control and stability. We have focused on self-assembled monolayers (SAMs) of porphyrins on flat gold substrates because they can provide densely packed, highly ordered structures of porphyrins on 2D gold electrodes suitable for developing artificial photosynthetic systems.[22,23] They include mixed SAMs of a pyrene or boron dipyrrin energy donor and porphyrin energy-acceptor systems, which exhibit efficient photoinduced energy transfer on the 2D gold surfaces, mimicking the light-harvesting function in antenna complexes.[22,23] In addition, boron dipyrrin as light-harvesting molecule has been combined with a charge-separation molecule, the ferrocene−porphyrin−fullerene triad, to construct integrated artificial photosynthetic assemblies on a gold electrode using mixed monolayers of the respective self-assembled unit (Figure 8).[22c] The mixed self-assembled monolayers on the gold electrode have established a cascade of photoinduced energy transfer and multistep electron transfer, leading to the production of photocurrent output with the highest internal quantum yield ($50 \pm 8\%$ based on the adsorbed photons) ever reported for photocurrent generation at monolayer-modified metal electrodes and across artificial membranes using donor−acceptor linked molecules.[22,23,44−46]

However, strong quenching of the porphyrin excited singlet state by gold surfaces[22a] has precluded the achievement of a high quantum yield for charge separation on the surfaces as attained in photosynthesis. Furthermore, the incident photon-to-photocurrent efficiency (IPCE), which is strongly associated with the light-harvesting efficiency in 2D systems, has been limited by the poor light-harvesting efficiency of the porphyrin monolayers.[22,23] To overcome these problems, a new type of artificial light-harvesting system, which remarkably enhances the light-harvesting properties, should be exploited to combine with the charge-separation system on the ITO electrode, which suppresses energy-transfer quenching. Metal nanoclusters, which can provide 3D architectures, seem to be good candidates for nanoscaffolds for antenna molecules.[46−48] In particular, alkanethiolate-monolayer-protected gold nanoclusters are stable in air and soluble in common organic solvents, being capable of facile modification with other functional thiols through exchange reactions or by couplings and nucleophilic substitutions.[47] Therefore, the construction of the 3D architectures of porphyrin-modified metal nanoclusters, which have large surface areas, on ITO electrodes would improve the light-harvesting efficiency as compared to that of the 2D porphyrin SAMs. Furthermore, the interaction of the porphyrin excited singlet state with metal nanoclusters would be reduced significantly, relative to the bulk gold surface, because of the "quantum effect".[48] In this context, multiporphyrin-monolayer-modified gold clusters (H_2PC11AuC) have been prepared as a new type of artificial photosynthetic material (Figure 9).[24,49−51] The photophysical and electrochemical properties of H_2PC11AuC are compared to those of the corresponding 2D porphyrin SAM (H_2PC11Au(111)), as shown in Figure 9.[24,49] H_2PC11AuC was directly synthesized by the reduction of $AuCl_4^-$ with $NaBH_4$ in toluene containing the corresponding porphyrin alkanethiol to avoid incomplete functionalization. H_2PC11AuC was purified repeatedly by gel permeation chromatography and characterized by ^{1}H NMR, UV−vis, and fluorescence spectroscopy, electrochemistry, elemental analysis, and transmission electron microscopy (TEM).[24,49]

The mean diameter of the gold core determined by TEM was 2.1 nm (with a standard deviation of $\sigma = 0.3$ nm) for H_2PC11AuC, which is similar to the value obtained for alkanethiolate-protected gold nanoclusters under the same experimental conditions. Taking the gold core as a sphere, the model predicts that the core of H_2PC11AuC contains 280 gold atoms, of which 143 lie on the gold surface. Given the values for the elemental analysis of H_2PC11AuC, there are 57 porphyrin alkanethiolate chains on the gold surface for H_2-PC11AuC. It should be emphaszied here that the molecular weight of H_2PC11AuC is estimated to be 120 000, which is one of the highest values for multiporphyrin arrays with well-defined structure. The coverage ratio of porphyrin alkanethiolate chains of H_2PC11AuC to surface gold atoms (γ) is determined to be 40%, which is remarkably larger than the coverage ratio ($\gamma = 6.5\%$) of 2D porphyrin SAM H_2PC11Au(111). In other words, the light-harvesting properties of the 3D system are much improved as compared to those of the 2D system. ^{1}H NMR, cyclic voltammetry, and absorption measurements of H_2-PC11AuC have revealed that the porphyrin environment of H_2-PC11AuC is virtually the same as that of the porphyrin reference compound (H_2P−NHCO-ref in Figure 9) in solution and is less perturbed than that of H_2PC11Au(111).[24,49]

To establish the excited-state deactivation pathways, nanosecond transient absorption spectra were recorded as the excitation of H_2PC11AuC and H_2P−NHCO-ref in benzonitrile. H_2PC11AuC and H_2P−NHCO-ref exhibit characteristic absorption due to the porphyrin excited triplet state, but the intensity of transient absorption for H_2PC11AuC is much lower than that of H_2P−NHCO-ref under the same experimental conditions. This implies that most of the porphyrin excited singlet state on the gold nanoparticles is quenched by the metal surface, whereas the residual porphyrin excited triplet state is generated via intersystem crossing from the unquenched porphyrin excited singlet state. Picosecond transient absorption spectra were also taken as the excitation of H_2PC11AuC in benzonitrile. Immediately after the excitation of H_2PC11AuC, transient absorption due to the porphyrin excited singlet state emerges. The rate constant for the decay of the band ($k_q = 7.7 \times 10^9$ s^{-1}) agrees well with the values for the rise of a hot band due to the surface plasmon[52] and the values for a short component of the fluorescence decay. These results indicate that the porphyrin excited singlet state in the present systems is quenched by the metal surface via energy transfer rather than electron transfer.[24,49] The fluorescence of 3D porphyrin H_2PC11AuC exhibits a double-exponential decay (0.13 ns (93%), 9.6 ns (7%)). The lifetime of the minor, longer-lived component of H_2PC11AuC in benzonitrile is close to that of the porphyrin reference (∼10 ns). This minor component may result from different ligation sites (vertex, edge, terrace, and defect) on the truncated

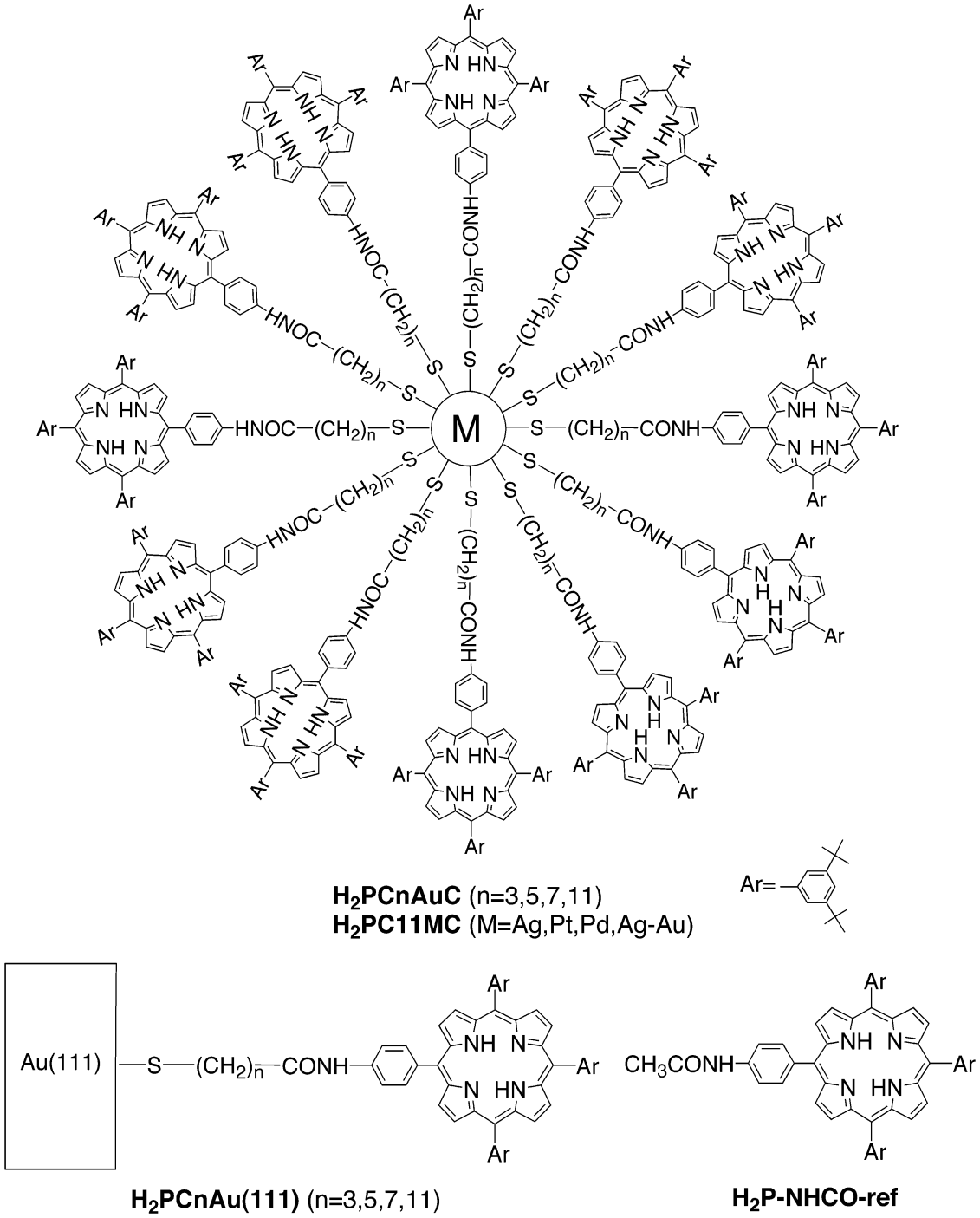

Figure 9. Schematic structures of porphyrin-modified metal nanoclusters H_2PCnAuC (n = 3, 5, 7, 11) and H_2PC11MC (M = Ag, Pt, Pd, Ag−Au) and porphyrin SAM on Au(111) (H_2PCnAu(111)) (n = 3, 5, 7, 11) and porphyrin reference H_2P−NHCO-ref.

octahedral Au-core surface. The lifetime of the major, short-lived component (0.13 ns (93%)) is significantly longer than that of H_2PC11Au(111) (0.040 ns). These results clearly demonstrate that the quenching of the porphyrin excited singlet state by the gold clusters via energy transfer is very much suppressed relative to the energy-transfer quenching by the bulk Au(111) surface.[24,49]

We have also prepared multiporphyrin-modified metal nanoclusters H_2PCnAuC with different spacer chain lengths to examine the effects of the chain length of the spacer (n = 3, 5, 7, 11) on the structure and photophysical properties (Figure 9).[49b] TEM data reveals that the size of the gold nanocluster is not affected by the chain length of the spacer, even in the case of the large porphyrin moiety. The TEM image of H_2PC3AuC exhibits hexagonal packing of H_2PC3AuC where the edge-to-edge separation distance between the gold core (3.6 nm) is 2 times larger than the thickness of the porphyrin monolayer. Such hexagonal packing of H_2PC3AuC can be ascribed to the densely packed, rigid structure of the porphyrin moieties near the gold nanocluster due to a short methylene spacer (n = 3).[49b] Although similar hexagonal packing was not seen for the other porphyrin-modified gold nanoclusters with longer spacers (n = 5, 7, 11), the separation distances between the gold core in the TEM images are largely similar, irrespective of the chain length of the spacer. Because the spacer is splayed outward from the highly curved outermost surface of the gold nanoclusters, the void space between the porphyrins increases with the increasing chain length of the spacer. This allows the porphyrin moieties

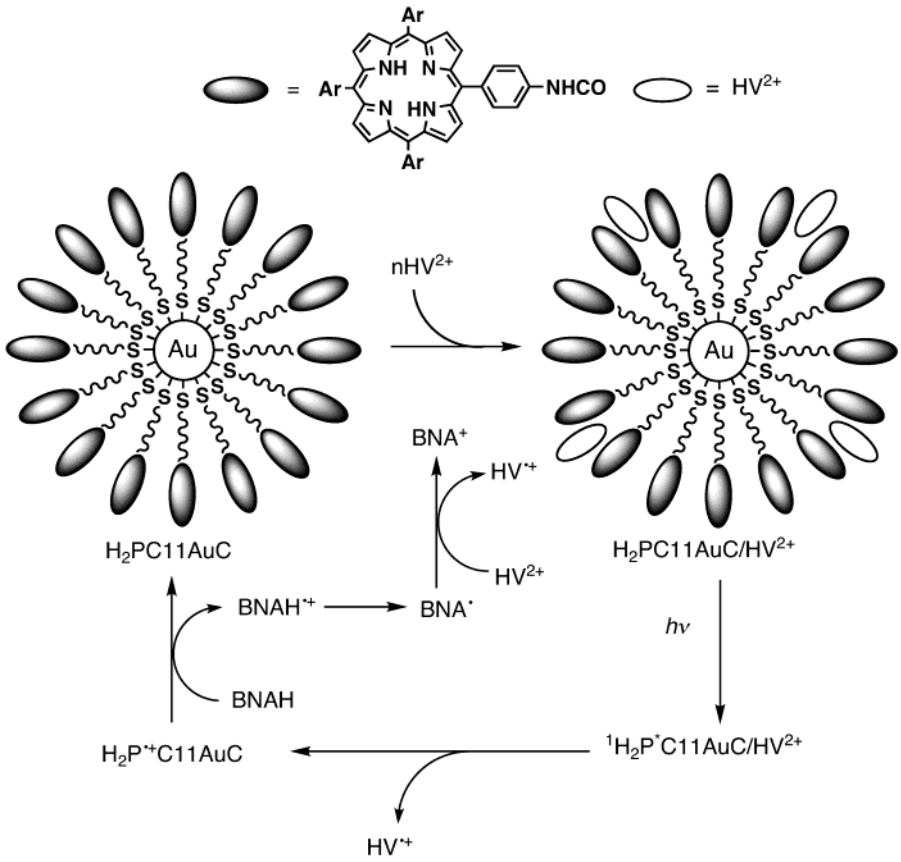

Figure 10. Mechanism of the $H_2PC11AuC$-photocatalyed reduction of HV^{2+} by BNAH.

to interpenetrate each other to leave the separation distance similar. The fluorescence lifetime slightly decreases with decreasing spacer length, which is in accordance with the quenching trend in the 2D porphyrin SAMs.[22a] Plots of ln k_q versus d (edge-to-edge distance) yield the same β value (damping factor) for $H_2PCnAuC$ and $H_2PCnAu(111)$, 0.1 ± 0.01 $Å^{-1}$. The energy-transfer rate of the 3D surface, which is slower than that of the 2D surface, may result from fewer gold atoms ($\sim 10^2$) on the 3D surface of the nanoparticles involved in energy transfer as compared to the number on the 2D surface of the bulk flat electrode. The β value in this study is remarkably small relative to those for conventional energy-transfer systems (0.3−1.7 $Å^{-1}$).[53] The small β value suggests that the alky chain is not fully extended as the chain length increases and that surface plasmons play an important role in fluorescence quenching because energy transfer from the exited fluorophore to the metal surface is known to be enhanced by surface plasmons and the energy transfer to surface plasmons is a slowly varying function of distance.[49b] However, the exact mechanism of fluorescence quenching remains to be clarified.[49b]

Three-dimensional porphyrin-monolayer-protected metal nanoclusters ($H_2PC11MC$) have been prepared to examine the effects of the metal (M = Au, Ag, Au−Ag alloy, Pd, and Pt) and the size (i.e., 1∼3 nm (M = Au)) on the structures and photophysical properties (Figure 9).[49a] The quenching rate constants of the porphyrin excited singlet state by the surfaces of monometal nanoclusters and gold nanoclusters with a different diameters are virtually the same. In contrast, the quenching rate constant of the gold−silver alloy nanocluster is 2 times smaller than that of the corresponding monometal clusters (i.e., Au or Ag). This reveals that the interaction between the surface of the gold−silver alloy and the porphyrin excited singlet state is reduced considerably in comparison to the interactions of the monometal systems. Accordingly, porphyrin metal alloy nanoclusters are potential candidates for a new type of artificial photosynthetic material and photocatalyst.[49a]

Because the porphyrin-modified metal nanoclusters possess highly efficient light-harvesting properties together with the suppression effect of energy-transfer quenching by the metal surface, they are also expected to exhibit efficient energy transfer from the zinc porphyrin excited singlet state to the free base porphyrin when mixed self-assembled monolayers of zinc porphyrins and free base porphyrins are made on the gold nanocluster. Preliminary experiments on the mixed system did not show any clear evidence of the energy-transfer process. No energy-transfer behavior is rationalized by the relatively large separation distance and the unfavorable parallel orientation between the porphyrins.

However, such morphology is highly favorable to the incorporation of a guest molecule (i.e., acceptor) between the porphyrins, exhibiting photocatalytic and photovoltaic functions. Bearing these in mind, the photocatalytic function of 3D porphyrin-monolayer-protected gold clusters with different chain lengths has been examined for the photocatalytic reduction of hexyl viologen (HV^{2+}) by 1-benzyl-1,4-dihydronicotinamide (BNAH) in comparison with that of the reference porphyrin compound without metal clusters (Figure 10).[50] Both porphyrin-monolayer-protected gold clusters and the reference porphyrin compound (H_2P−NHCO-ref) act as efficient photocatalysts for the uphill reduction of HV^{2+} by BNAH to produce the 1-benzylnicotinamidinium ion (BNA^+) and the hexyl viologen radical cation ($HV^{\bullet+}$) in benzonitrile. In the case of porphyrin-monolayer-protected gold clusters, the quantum yield reaches a maximum value with an extremely low concentration of HV^{2+}, which is larger than the corresponding value of the H_2P−NHCO-ref system. The dependence of quantum yields on

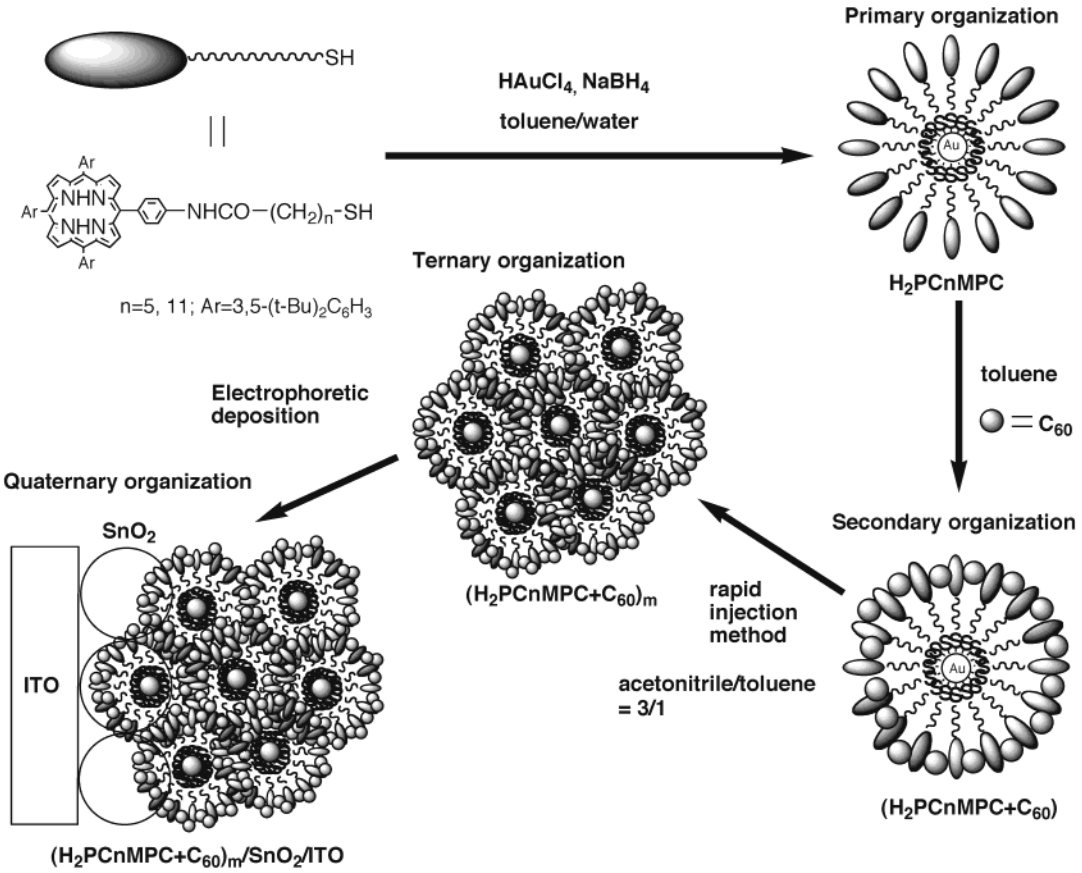

Figure 11. Schematic view of the quaternary self-organization of porphyrin and fullerene units by clusterization with gold nanoparticles on nanostructured SnO_2 electrodes for organic photovoltaic devices.

concentrations of BNAH and HV^{2+} as well as on the time-resolved single-photon counting fluorescence and transient absorption spectroscopic results indicates that the photoinduced electron transfer from the triplet excited state of H_2P−NHCO-ref to HV^{2+} initiates the photocatalytic reduction of HV^{2+} by BNAH but that the photoinduced electron transfer from the singlet excited state of porphyrin-monolayer-protected gold clusters to HV^{2+}, which forms a supramolecular complex with them, is responsible for the photocatalytic reaction. Intersystem crossing from the porphyrin singlet excited state to the triplet excited state is very much suppressed by the quenching of the porphyrin excited singlet state via energy transfer to the gold surface of the 3D porphyrin-modified gold nanoclusters. However, the 3D architectures of porphyrin-modified gold nanoclusters with a suitable cleft between the porphyrin moieties allow us to interact HV^{2+} with them, resulting in fast electron transfer from the singlet excited state of porphyrin to HV^{2+} on porphyrin-modified gold nanoclusters.[50]

The successful construction of the photocatalytic system using multiporphyrin-modified gold nanoclusters and the hexylviolgen acceptor has encouraged us to design novel organic solar cells prepared using the quaternary self-organization of porphyrin (donor) and fullerene (acceptor) dye units by clusterization with gold nanoparticles on SnO_2 electrodes, as in the case of multiporphyrin dendrimers (Figure 11).[51] First, porphyrin−alkanethiolate-monolayer-protected gold nanoclusters with a well-defined size (8−9 nm) and spherical shape (H_2PCnAuC (n = 5, 11)) are prepared starting from porphyrin−alkanethiol (primary organization). These nanoparticles form complexes with fullerene molecules, which are incorporated between the porphyrin moieties (secondary organization), and they form clusters in an acetonitrile/toluene mixed solvent (ternary organization). Then, the clusters are associated onto SnO_2 electrodes by an electrophoretic deposition method that makes large clusters on the electrode surface (quaternary organization), as in the case of supramolecular organic solar cells of multiporphyrin dendrimers and fullerenes.[51]

The quaternary organization of H_2PCnAuC and C_{60} composite clusters (denoted as $(H_2PCnAuC + C_{60})_m$ (n = 5, 11)) was induced by injecting a mixed toluene solution of H_2PCnAuC and C_{60} in acetonitrile/toluene (3:1 v/v). This procedure allows us to achieve complex formation between H_2PCnAuC and C_{60} and clusterization simultaneously. The clusterization of the H_2-PCnAuC reference system without C_{60} (denoted as $(H_2PCnAuC)_m$ (n = 5, 11)) or the porphyrin and C_{60} reference system without gold nanoparticles (denoted as $(H_2P\text{-ref} + C_{60})_m$) was also performed in the same manner. The absorption spectra of $(H_2PC11AuC + C_{60})_m$ and $(H_2PC11AuC)_m$ in a 3:1 acetonitrile/toluene mixture are much broader than those in toluene, implying the cluster formation in the mixed solvent.[51]

The TEM image of $(H_2PC11AuC + C_{60})_m$ displays the well-controlled size and shape of larger nanoclusters with a diameter of 300−400 nm. These clusters are in sharp contrast to the TEM image of $(H_2PC11AuC)_m$ without C_{60}, exhibiting a smaller, irregular size. Judging from the diameter of H_2PCnAuC (8−9 nm), one can safely conclude that H_2PCnAuC clusters are self-assembled with C_{60} molecules in the mixed solution to yield larger donor−acceptor (D−A) nanoclusters with an interpenetrating network. Upon subjecting the resultant cluster suspension to a high electric dc field, mixed H_2PCnAuC and C_{60} clusters ($(H_2PCnAuC + C_{60})_m$) and reference clusters ($(H_2$-PCnAuC$)_m$ or $(H_2P\text{-ref} + C_{60})_m$) were deposited onto an ITO of a nanostructured SnO_2 electrode (ITO/SnO_2) to give modified electrodes (denoted as ITO/SnO_2/$(H_2PCnAuC + C_{60})_m$, ITO/

$SnO_2/(H_2PCnAuC)_m$, and ITO/SnO_2/(H_2P-ref + $C_{60})_m$ (n = 5, 11)), respectively. The absorptivity of ITO/SnO_2/($H_2PCnAuC + C_{60})_m$ is very much enhanced as compared with that of ITO/$SnO_2/(H_2PCnAuC)_m$. These results ensure that the incident light is absorbed intensively in the visible and near-IR regions by ITO/$SnO_2/(H_2PCnAuC + C_{60})_m$. The AFM image of ITO/$SnO_2$/($H_2PC11MPC + C_{60})_m$ and ITO/$SnO_2/(H_2PC11AuC)_m$ reveals cluster aggregation with a regular size. These results also suggest that the electric deposition of ($H_2PCnAuC + C_{60})_m$ and (H_2-$PCnAuC)_m$ leads to the association of smaller clusters on nanostructured SnO_2 electrode to grow larger ones. ITO/SnO_2/($H_2PC11AuC + C_{60})_m$ (700−900 nm) is much larger than ITO/$SnO_2/(H_2PC11AuC)_m$ (300−400 nm). This indicates that quaternary organization of the porphyrin and C_{60} molecules is achieved on SnO_2, allowing the formation of an interpenetrating network of the porphyrin and C_{60} molecules for ITO/SnO_2/(H_2-$PCnAuC + C_{60})_m$.[51]

Photoelectrochemical measurements were performed with a standard two-electrode system, as in the case of ITO/SnO_2/($DnH_2Pn + C_{60})_m$/NaI + I_2/Pt devices (vide supra). The IPCE value of the ITO/$SnO_2/(H_2PC11AuC)_m$/NaI + I_2/Pt device exhibits a remarkable increase with the increasing relative ratio of C_{60} to reach a maximum IPCE of 28% at 490 nm with an initial relative ratio of $[H_2P]/[C_{60}]$ = 37:63. Taking into account the well-established photodynamics of the porphyrin−fullerene system,[4,31] these results lead to the conclusion that the porphyrin excited singlet state is quenched rapidly by C_{60} via electron transfer in the porphyrin−C_{60} complex rather than by the gold nanocluster via energy transfer. This is consistent with the results that under the same conditions the IPCE value is 7 times larger than that of the ITO/SnO_2/($H_2PC5AuC + C_{60})_m$/NaI + I_2/Pt device, where the chain length of $H_2PC5AuC$ is too short to accommodate C_{60} between two porphyrin rings. In this case, the porphyrin excited singlet state is quenched more efficiently by the gold nanocluster because of the short spacer (i.e., n = 5) between the porphyrin and the gold nanocluster rather than electron transfer to C_{60}.[51]

The ITO/SnO_2/($H_2PC11AuC + C_{60})_m$/NaI + I_2/Pt device has a fill factor (FF) of 0.35, an open-circuit voltage (V_{OC}) of 420 mV, a short-circuit current density (I_{SC}) of 0.14 mA cm^{-2}, and an overall power conversion efficiency (η) of 0.61% at an input power (W_{IN}) of 3.4 mW cm^{-2}. The η value (0.61%) of the ITO/SnO_2/($H_2PC11AuC + C_{60})_m$/NaI + I_2/Pt device is also remarkably enhanced in comparison with the values of the OTE/SnO_2/($D4H_2P4 + C_{60})_m$/NaI + I_2/Pt (0.32%) and ITO/SnO_2/(H_2P-ref + $C_{60})_m$/NaI + I_2/Pt devices under the same experimental conditions. Furthermore, the IPCE value obtained with the ITO/SnO_2/($H_2PC11AuC + C_{60})_m$/NaI + I_2/Pt device is more than an order of magnitude greater than the value obtained with the ITO/$TiO_2/(H_2P\text{-ref})_m$/NaI + I_2/Pt device. These results clearly show the large improvement in the photoelectrochemical properties results from the 3D structure of the interpenetrating network of the porphyrin and C_{60} molecules in the present system.[51]

The photocurrent-generation mechanism in the present device is proposed as follows (Figure 7). First, photoinduced electron transfer takes place from the porphyrin excited singlet state ($^1H_2P^*/H_2P^{\bullet+}$ = −0.7 V vs NHE) to C_{60} ($C_{60}/C_{60}^{\bullet-}$ = −0.2 V vs NHE) in the porphyrin−C_{60} complex, followed by electron injection from $C_{60}^{\bullet-}$ to the conduction band of SnO_2 (0 V vs NHE) to yield the porphyrin radical cation and a separated electron within the SnO_2 nanocrystallites. The porphyrin radical cation ($H_2P/H_2P^{\bullet+}$ = 1.2 V vs NHE) captures an electron from the iodide (I^-/I_3^- = 0.5 V vs NHE) in the electrolyte system to generate photocurrent.[51]

A remarkable enhancement in the photoelectrochemical performance and the broader photoresponse in the visible and IR regions relative to the reference systems demonstrate the fact that the quaternary organization approach provides a novel perspective on the development of efficient organic solar cells. The suitable and similar geometry between the porphyrin and fullerene within the porphyrin-modified gold nanocluster may be responsible for the good performance of the present organic photovoltaic device.

3. Conclusions and Outlook

Synthetic giant multiporphyrin arrays have been found to be artificial mimics of light-harvesting systems. Meso,meso-linked porphyrin oligomers have been successfully incorporated into multistep electron-transfer systems to realize both light-harvesting and charge-separation functions in the light-harvesting complexes and the reaction center. In particular, the ferrocene-meso,meso-linked porphyrin trimer−fullerene pentad reveals the formation of an extremely long-lived charge-separated state (0.53 s) with a high quantum yield (0.83), which is comparable to the natural photosynthetic system. Multiporphyrin dendrimers as light-harvesting materials are also shown to be attractive building blocks for the construction of organic solar cells. Finally, we have successfully prepared novel multiporphyrin-modified metal nanoclusters that have improved light-harvesting properties and suppress the undesirable energy-transfer quenching of the porphyrin excited singlet state by the metal surface. Because multiporphyrin-modified metal nanoclusters have flexible molecular-recognition clefts between the porphyrins, they can be combined with acceptors (viologens or fullerenes) to exhibit photocatalytic or photovoltaic properties. In particular, multiporphyrin-modified gold nanoclusters have been assembled with fullerenes step-by-step to make large, uniform clusters on nanostructured semiconductor electrodes, which have a high power-conversion efficiency close to 1%. The power-conversion efficiency of our device (∼1%) is still lower than that of inorganic solar cells at present. Nevertheless, the performance of the present cells may be improved by modulating the molecular structure and electronic properties of the porphyrin and fullerene, the nature of the spacer and by selecting suitable substrates as electrodes as well as integrating novel multiporphyrin-based light-harvesting systems. Although the relatively high value is undoubtedly associated with the small reorganizational energies of porphyrins and fullerenes, the 3D fabrication of nanostructures in the solid state (i.e., the nanohighway for electron and hole injection to respective electrodes) may also be crucial to further improvement.

Multiporphyrins-based nanoarchitecture with well-defined structures will open the door to nanoscience and nanotechnology, which cross a variety of fields including chemistry, biology, physics, and electronics, to develop new scientific principles and concepts.

Acknowledgment. This work was supported in part by the Kyoto University Alliance for Chemistry (COE Program of the Ministry of Education, Culture, Sports, Science and Technology, Japan). We are indebted to our colleagues and co-workers cited in the references, particularly Yoshiteru Sakata, Shunichi Fukuzumi, Tadashi Okada, Iwao Yamazaki, Osamu Ito, Dirk M. Guldi, Nikolai V. Tkachenko, Helge Lemmetyinen, Prashant V. Kamat, Dongho Kim, Maxwell J. Crossley, and Hiroko Yamada, for much of the work that is contained herein.

References and Notes

(1) (a) Wasielewski, M. R. *Chem. Rev.* **1992**, *92*, 435. (b) Gust, D.; Moore, T. A.; Moore, A. L. *Acc. Chem. Res.* **1993**, *26*, 198. (c) Kurreck, H.; Huber, M. *Angew. Chem., Int. Ed. Engl.* **1995**, *34*, 849. (d) Gust, D.; Moore, T. A. In *The Porphyrin Handbook*; Kadish, K. M., Smith, K., Guilard, R., Eds.; Academic Press: San Diego, CA, 2000; Vol. 8, pp 153−190. (e) Gust, D.; Moore, T. A.; Moore, A. L. *Acc. Chem. Res.* **2001**, *34*, 40. (f) Adams, D. M.; Brus, L.; Chidsey, E. D.; Creager, S.; Creutz, C.; Kagan, C. R.; Kamat, P. V.; Lieberman, M.; Lindsey, S.; Marcus, R. A.; Metzger, R. M.; Michel-Beyerle, M. E.; Miller, J. R.; Newton, M. D.; Rolison, D. R.; Sankey, O.; Schanze, K. S.; Yardley, J.; Zhu, X. *J. Phys. Chem. B* **2003**, *107*, 6668.

(2) (a) Harriman, A.; Sauvage, J.-P. *Chem. Soc. Rev.* **1996**, 41. (b) Blanco, M.-J.; Jiménez, M. C.; Chambron, J.-C.; Heitz, V.; Linke, M.; Sauvage, J.-P. *Chem. Soc. Rev.* **1999**, 293. (c) Balzani, V.; Juris, A.; Venturi, M.; Campagna, S.; Serroni, S. *Chem. Rev.* **1996**, *96*, 759. (d) *Electron Transfer in Chemistry*; Balzani, V., Ed.; Wiley-VCH: Weinheim, Germany, 2001. (e) Armaroli, N. *Photochem. Photobiol. Sci.* **2003**, *2*, 73. (f) *Molecular Electronics*; Jortner, J., Ratner, M., Eds.; Blackwell: London, 1997.

(3) (a) Paddon-Row, M. N. *Acc. Chem. Res.* **1994**, *27*, 18. (b) Verhoeven, J. W. *Adv. Chem. Phys.* **1999**, *106*, 603. (c) Maruyama, K.; Osuka, A.; Mataga, N. *Pure Appl. Chem.* **1994**, *66*, 867. (d) Osuka, A.; Mataga, N.; Okada, T. *Pure Appl. Chem.* **1997**, *69*, 797. (e) Sun, L.; Hammarström, L.; Åkermark, B.; Styring, S. *Chem. Soc. Rev.* **2001**, 36. (f) Holten, D.; Bocian, D. F.; Lindsey, J. S. *Acc. Chem. Res.* **2002**, *35*, 57.

(4) (a) Imahori, H.; Sakata, Y. *Adv. Mater.* **1997**, *9*, 537. (b) Imahori, H.; Sakata, Y. *Eur. J. Org. Chem.* **1999**, 2445. (c) Imahori, H.; Mori, Y.; Matano, Y. *J. Photochem. Photobiol., C* **2003**, *4*, 51. (d) Guldi, D. M. *Chem. Commun.* **2000**, 321. (e) Guldi, D. M.; Prato, M. *Acc. Chem. Res.* **2000**, *33*, 695.

(5) (a) *The Photosynthetic Reaction Center*; Deisenhofer, J., Norris, J. R., Eds.; Academic Press: San Diego, CA, 1993. (b) *Anoxygenic Photosynthetic Bacteria*; Blankenship, R. E., Madigan, M. T., Bauer, C. E., Eds.; Kluwer Academic Publishing: Dordrecht, The Netherlands, 1995.

(6) (a) McDermott, G.; Prince, S. M.; Freer, A. A.; Hawthornthwaite-Lawless, A. M.; Papiz, M. Z.; Cogdell, R. J.; Isaacs, N. W. *Nature* **1995**, *374*, 517. (b) Papiz, M. Z.; Prince, S. M.; Howard, R. J.; Cogdell, N. W.; Isaacs, N. W. *J. Mol. Biol.* **2003**, *326*, 1523. (c) Roszak, A. W.; Howard, T. D.; Southall, J.; Gardiner, A. T.; Law, C. J.; Isaacs, N. W.; Cogdell, R. J. *Science* **2003**, *302*, 1969.

(7) (a) Deisenhofer, J.; Epp, O.; Miki, K.; Huber, R.; Michel, H. *Nature* **1985**, *318*, 618. (b) Fritzsch, G.; Koepke, J.; Diem, R.; Kuglstatter, A.; Baciou, L. *Acta Crystallogr., Sect. D* **2002**, *58*, 1660.

(8) Olson, J. M. *Photochem. Photobiol.* **1998**, *67*, 61.

(9) (a) Zouni, A.; Witt, H.-T.; Kern, J.; Fromme, P.; Kraub, N.; Saenger, W.; Orth, P. *Nature* **2001**, *409*, 739. (b) Jordan, P.; Fromme, P.; Witt, H.-T.; Klukas, O.; Saenger, W.; Kraub, N. *Nature* **2001**, *411*, 909.

(10) Ben-Shem, A.; Frolow, F.; Nelson, N. *Nature* **2003**, *426*, 630.

(11) (a) Prathapan, S.; Johnson, T. E.; Lindsey, J. S. *J. Am. Chem. Soc.* **1993**, *115*, 7519. (b) Wagner, R. W.; Johnson, T. E.; Lindsey, J. S. *J. Am. Chem. Soc.* **1996**, *118*, 11166. (c) Li, J.; Ambroise, A.; Yang, S. I.; Diers, J. R.; Seth, J.; Wack, C. R.; Bocian, D. F.; Holten, D.; Lindsey, J. S. *J. Am. Chem. Soc.* **1999**, *121*, 8927. (d) Lammi, R. K.; Ambroise, A.; Balasubramanian, T.; Wagner, R. W.; Bocian, D. F.; Holten, D.; Lindsey, J. S. *J. Am. Chem. Soc.* **2000**, *122*, 7579. (e) Kuciauskas, D.; Liddell, P. A.; Lin, S.; Johnson, T. E.; Weghorn, S. J.; Lindsey, J. S.; Moore, A. L.; Moore, T. A.; Gust, D. *J. Am. Chem. Soc.* **1999**, *121*, 8604.

(12) (a) Maruyama, K.; Osuka, A. *Pure Appl. Chem.* **1990**, *62*, 1511. (b) Nagata, T.; Osuka, A.; Maruyama, K. *J. Am. Chem. Soc.* **1990**, *112*, 3054. (c) Osuka, A.; Tanabe, N.; Nakajima, S.; Maruyama, K. *J. Chem. Soc., Perkin Trans. 2* **1996**, 199.

(13) (a) Mongin, O.; Schuwey, A.; Vallot, M. A.; Gossauer, A. *Tetrahedron Lett.* **1999**, *121*, 8927. (b) Solladié, N.; Gross, M.; Gisselbrecht, J.-P.; Sooambar, C. *Chem. Commun.* **2001**, 2206. (c) Slone, R. V.; Hupp, J. T. *Inorg. Chem.* **1997**, *36*, 5422. (d) Prodi, A.; Indelli, M. T.; Kleverlaan, C. J.; Scandola, F.; Alessio, E.; Gianferrara, T.; Marzilli, L. G. *Chem.−Eur. J.* **1999**, *5*, 2668.

(14) (a) Crossley, M. J.; Burn, P. L. *J. Chem. Soc., Chem. Commun.* **1991**, 1569. (b) Crossley, M. J.; Govenlock, L. J.; Prashar, J. K. *J. Chem. Soc., Chem. Commun.* **1995**, 2379. (c) Officer, D. L.; Burrell, A. K.; Reid, D. C. W. *Chem. Commun.* **1996**, 1657. (d) Vicente, M. G. H.; Cancilla, M. T.; Lebrilla, C. B.; Smith, K. M. *Chem. Commun.* **1998**, 1261. (e) Vincente, M. G. H.; Jaquinod, L.; Smith, K. M. *Chem. Commun.* **1999**, 1771. (f) Burrell, A. K.; Officer, D. L.; Plieger, P. G.; Reid, D. C. W. *Chem. Rev.* **2001**, *101*, 2751.

(15) (a) Lin, V. S.-Y.; DiMagno, S. G.; Therien, M. J. *Science* **1994**, *264*, 1105. (b) Lin, V. S.-Y.; Therien, M. J. *Chem.−Eur. J.* **1995**, *1*, 645. (c) Fletcher, J. T.; Therien, M. J. *J. Am. Chem. Soc.* **2000**, *122*, 12393. (d) Susumu, K.; Therien, M. J. *J. Am. Chem. Soc.* **2002**, *124*, 8550.

(16) (a) Anderson, H. L.; Martin, S. J.; Bradley, D. D. C. *Angew. Chem., Int. Ed. Engl.* **1994**, *33*, 655. (b) Anderson, H. L. *Inorg. Chem.* **1994**, *33*, 972. (c) Anderson, H. L.; Anderson, S.; Sanders, J. K. M. *J. Chem. Soc., Perkin Trans. 1* **1995**, 2231. (d) Screen, T. E. O.; Thorne, J. R. G.; Denning, R. G.; Bucknall, D. G.; Anderson, H. L. *J. Am. Chem. Soc.* **2002**, *124*, 9712. (e) Mak, C. C.; Bampos, N.; Sanders, J. K. M. *Angew. Chem., Int. Ed.* **1998**, *37*, 3020.

(17) (a) Anderson, S.; Anderson, H. L.; Sanders, J. K. M. *Angew. Chem., Int. Ed. Engl.* **1992**, *31*, 907. (b) Anderson, S.; Anderson, H. L.; Bashall, A.; McPartlin, M.; Sanders, J. K. M. *Angew. Chem., Int. Ed. Engl.* **1995**, *34*, 1096. (c) Hyacock, R. A.; Yartsev, A.; Michelson, U.; Sundström, V.; Hunter, C. A. *Angew. Chem., Int. Ed.* **2000**, *39*, 3616. (d) Kuroda, Y.; Sugou, K.; Sasaki, K. *J. Am. Chem. Soc.* **2000**, *122*, 7833. (e) Sugou, K.; Sasaki, K.; Kitayama, K.; Iwaki, T.; Kuroda, Y. *J. Am. Chem. Soc.* **2002**, *124*, 1182.

(18) (a) Aratani, N.; Osuka, A. *Bull. Chem. Soc. Jpn.* **2001**, *74*, 1361. (b) Aratani, N.; Osuka, A.; Cho, H. S.; Kim, D. *J. Photochem. Photobiol. C* **2002**, *3*, 25. (c) Kim, D.; Osuka, A. *J. Phys. Chem. A* **2003**, *107*, 8791.

(19) (a) Sugiura, K.; Tanaka, H.; Matsumoto, T.; Kawai, T.; Sakata, Y. *Chem. Lett.* **1999**, 1193. (b) Benites, M. R.; Johnson, T. E.; Weghorn, S.; Yu, L.; Rao, P. D.; Diers, J. R.; Yang, S. I.; Kirmaier, C.; Bocian, D. F.; Holten, D.; Lindsey, J. S. *J. Mater. Chem.* **2002**, *12*, 65.

(20) (a) Choi, M.-S.; Aida, T.; Yamazaki, T.; Yamazaki, I. *Angew. Chem., Int. Ed.* **2001**, *40*, 3194. (b) Choi, M.-S.; Aida, T.; Yamazaki, T.; Yamazaki, I. *Chem.−Eur. J.* **2002**, *8*, 2667. (c) Choi, M.-S.; Aida, T.; Luo, H.; Araki, Y.; Ito, O. *Angew. Chem., Int. Ed.* **2003**, *42*, 4060. (d) Choi, M.-S.; Yamazaki, T.; Yamazaki, I.; Aida, T. *Angew. Chem., Int. Ed.* **2004**, *43*, 150.

(21) (a) Kato, T.; Maruo, N.; Akisada, H.; Arai, T.; Nishino, N. *Chem. Lett.* **2000**, 890. (b) Yeow, E. K. L.; Ghiggino, K. P.; Reek, J. N. H.; Crossley, M. J.; Bosman, A. W.; Schenning, A. P. H. J.; Meijer, E. W. *J. Phys. Chem. B* **2000**, *104*, 2596.

(22) (a) Imahori, H.; Norieda, H.; Nishimura, Y.; Yamazaki, I.; Higuchi, K.; Kato, N.; Motohiro, T.; Yamada, H.; Tamaki, K.; Arimura, M.; Sakata, Y. *J. Phys. Chem. B* **2000**, *104*, 1253. (b) Imahori, H.; Yamada, H.; Nishimura, Y.; Yamazaki, I.; Sakata, Y. *J. Phys. Chem. B* **2000**, *104*, 2099. (c) Imahori, H.; Norieda, H.; Yamada, H.; Nishimura Y.; Yamazaki, I.; Sakata, Y.; Fukuzumi, S., *J. Am. Chem. Soc.* **2001**, *123*, 100. (d) Yamada, H.; Imahori, H.; Nishimura, Y.; Yamazaki, I.; Fukuzumi, S. *Adv. Mater.* **2002**, *14*, 892. (e) Yamada, H.; Imahori, H.; Nishimura, Y.; Yamazaki, I.; Ahn, T. K.; Kim, S. K.; Kim, D.; Fukuzumi, S. *J. Am. Chem. Soc.* **2003**, *125*, 9129.

(23) (a) Uosaki, K.; Kondo, T.; Zhang, X.-Q.; Yanagida, M. *J. Am. Chem. Soc.* **1997**, *119*, 8367. (b) Kondo, T.; Kanai, T.; Iso-o, K.; Uosaki, K. *Z. Phys. Chem.* **1999**, *212*, 23.

(24) (a) Imahori, H.; Arimura, M.; Hanada, T.; Nishimura, Y.; Yamazaki, I.; Sakata, Y.; Fukuzumi, S. *J. Am. Chem. Soc.* **2001**, *123*, 335. (b) Imahori, H.; Fukuzumi, S. *Adv. Mater.* **2001**, *13*, 1197.

(25) (a) Tamiaki, H.; Miyatake, T.; Tanikaga, R.; Holzwarth, A. R.; Schaffner, K. *Angew. Chem., Int. Ed. Engl.* **1996**, *35*, 772. (b) Haycock, R. A.; Hunter, C. A.; James, D. A.; Michelsen, U.; Sutton, L. R. *Org. Lett.* **2000**, *2*, 2435. (c) Ogawa, K.; Kobuke, Y. *Angew. Chem., Int. Ed.* **2000**, *39*, 4070. (d) Takahashi, R.; Kobuke, Y. *J. Am. Chem. Soc.* **2003**, *125*, 2372. (e) Ballester, P.; Gomila, R. M.; Hunter, C. A.; King, A. S. H.; Twyman, L. J. *Chem. Commun.* **2003**, 38.

(26) (a) Drain, C. M.; Lehn, J.-M. *J. Chem. Soc., Chem. Commun.* **1994**, 2313. (b) Fan, J.; Whiteford, J. A.; Olenyuk, B.; Levin, M. D.; Stang, P. J.; Fleischer, E. B. *J. Am. Chem. Soc.* **1999**, *121*, 2741. (c) Kumar, R. K.; Balasubramanian, S.; Goldberg, I. *Inorg. Chem.* **1998**, *37*, 541. (d) Imamura, T.; Fukushima, K. *Coord. Chem. Rev.* **2000**, *198*, 133.

(27) (a) Osuka, A.; Shimidzu, H. *Angew. Chem., Int. Ed. Engl.* **1997**, *36*, 135. (b) Aratani, N.; Osuka, A.; Kim, Y. H.; Jeong, D. H.; Kim, D. *Angew. Chem., Int. Ed.* **2000**, *39*, 1458. (c) Kim, Y. H.; Jeong, D. H.; Kim, D.; Jeoung, S. C.; Cho, H. S.; Kim, S. K.; Aratani, N.; Osuka, A. *J. Am. Chem. Soc.* **2001**, *123*, 76.

(28) Aratani, N.; Cho, H. S.; Ahn, T. K.; Cho, S.; Kim, D.; Sumi, H.; Osuka, A. *J. Am. Chem. Soc.* **2003**, *125*, 9668.

(29) (a) Nakano, A.; Osuka, A.; Yamazaki, I.; Yamazaki, T.; Nishimura, Y. *Angew. Chem., Int. Ed.* **1999**, *38*, 1350. (b) Nakano, A.; Yamazaki, T.; Nishimura, Y.; Yamazaki, I.; Osuka, A. *Chem.−Eur. J.* **2000**, *6*, 3254. (c) Nakano, A.; Osuka, A.; Yamazaki, T.; Nishimura, Y.; Akimoto, S.; Yamazaki, I.; Itaya, A.; Murakami, M.; Miyasaka, H. *Chem.−Eur. J.* **2001**, *7*, 3134.

(30) (a) Bonifazi, D.; Diederlich, F. *Chem. Commun.* **2002**, 2178. (b) Bonifazi, D.; Scholl, M.; Song, F.; Echegoyen, L.; Accorsi, G.; Armaroli, N.; Diederich, F. *Angew. Chem., Int. Ed.* **2003**, *42*, 4966.

(31) (a) Imahori, H.; Tamaki, K.; Guldi, D. M.; Luo, C.; Fujitsuka, M.; Ito, O.; Sakata, Y.; Fukuzumi, S. *J. Am. Chem. Soc.* **2001**, *123*, 2607. (b) Imahori, H.; Tamaki, K.; Araki, Y.; Sekiguchi, Y.; Ito, O.; Sakata, Y.; Fukuzumi, S. *J. Am. Chem. Soc.* **2002**, *124*, 5165. (c) Imahori, H.; Sekiguchi, Y.; Kashiwagi, Y.; Sato, T.; Araki, Y.; Ito, O.; Yamada, H.; Fukuzumi, S. *Chem.−Eur. J.* **2004**, *10*, in press.

(32) (a) Hasobe, T.; Imahori, H.; Yamada, H.; Sato, T.; Fukuzumi, S. *Nano Lett.* **2003**, *3*, 409. (b) Hasobe, T.; Imahori, H.; Yamada, H.; Fukuzumi, S. *J. Porphyrins Phthalocyanines* **2003**, *7*, 296. (c) Fukuzumi, S.; Endo, Y.; Imahori, H. *J. Am. Chem. Soc.* **2002**, *124*, 10974.

(33) (a) Tomalia, D. A.; Baker, H.; Dewald, J.; Hall, M.; Kallos, G.; Martin, S.; Roeck, J.; Ryder, J.; Smith, P. *Polym. J.* **1985**, *17*, 117. (b) Newkome, G. R.; Moorefield, C. N.; Vögtle, F. *Dendritic Molecules: Concepts, Syntheses, Perspectives*; VCH: Weinheim, Germany, 1996.

(34) (a) O'Regan, B.; Grätzel, M. *Nature* **1991**, *335*, 737. (b) Hagfeldt, A.; Grätzel, M. *Chem. Rev.* **1995**, *95*, 49. (c) Hagfeldt, A.; Grätzel, M. *Acc. Chem. Res.* **2000**, *33*, 269. (d) Grätzel, M. *Nature* **2001**, *414*, 338. (e) Bignozzi, C. A.; Argazzi, R.; Kleverlaan, C. J. *Chem. Soc. Rev.* **2000**, *29*, 87.

(35) (a) Tang, C. W. *Appl. Phys. Lett.* **1986**, *48*, 183. (b) Granström, M.; Petritsch, K.; Arias, A. C.; Lux, A.; Andersson, M. R.; Friend, R. H. *Nature* **1998**, *395*, 257. (c) Huynh, W. U.; Dittmer, J. J.; Alivisatos, A. P. *Science* **2002**, *295*, 2425.

(36) (a) Halls, J. J. M.; Walsh, C. A.; Greenham, N. C.; Marseglia, E. A.; Friend, R. H.; Moratti, S. C.; Holmes, A. B. *Nature* **1995**, *376*, 498. (b) Schmidt-Mende, L.; Fechtenkötter, A.; Müllen, K.; Moons, E.; Friend, R. H.; MacKenzie, J. D. *Science* **2001**, *293*, 1119. (c) Yu, G.; Gao, J.; Hummelen, J. C.; Wudl, F.; Heeger, A. J. *Science* **1995**, *270*, 1789.

(37) (a) Brabec, C. J.; Sariciftci, N. S.; Hummelen, J. C. *Adv. Funct. Mater.* **2001**, *11*, 15. (b) Shaheen, S. E.; Brabec, C. J.; Sariciftci, N. S.; Padinger, F.; Fromherz, T.; Hummelen, J. C. *Appl. Phys. Lett.* **2001**, *78*, 841. (c) Padinger, F.; Rittberger, R. S.; Sariciftci, N. S. *Adv. Funct. Mater.* **2003**, *13*, 85. (d) Wienk, M. M.; Kroon, J. M.; Verhees, W. J. H.; Knol, J.; Hummelen, J. C.; van Hal, P. A.; Janssen, R. A. J. *Angew. Chem., Ind. Ed.* **2003**, *42*, 3371. (e) Eckert, E.-F.; Nicoud, J.-F.; Nierengarten, J.-F.; Liu, S.-G.; Echegoyen, L.; Barigelletti, F.; Armaroli, N.; Ouali, L.; Krasnikov, V.; Hadziioannou, G. *J. Am. Chem. Soc.* **2000**, *122*, 7467.

(38) (a) Imahori, H.; Hagiwara, K.; Akiyama, T.; Aoki, M.; Taniguchi, S.; Okada, T.; Shirakawa, M.; Sakata, Y. *Chem. Phys. Lett.* **1996**, *263*, 545. (b) Imahori, H.; Tkachenko, N. V.; Vehmanen, V.; Tamaki, K.; Lemmetyinen, H.; Sakata, Y.; Fukuzumi, S. *J. Phys. Chem. A* **2001**, *105*, 1750. (c) Vehmanen, V.; Tkachenko, N. V.; Imahori, H.; Fukuzumi, S.; Lemmetyinen, H. *Spectrochim. Acta, Part A* **2001**, 57, 2229. (d) Imahori, H.; Yamada, H.; Guldi, D. M.; Endo, Y.; Shimomura, A.; Kundu, S.; Yamada, K.; Okada, T.; Sakata, Y.; Fukuzumi, S. *Angew. Chem., Int. Ed.* **2002**, *41*, 2344. (e) Fukuzumi, S.; Ohkubo, K.; Imahori, H.; Guldi, D. M. *Chem.—Eur. J.* **2003**, *9*, 1585.

(39) (a) Imahori, H.; Hagiwara, K.; Aoki, M.; Akiyama, T.; Taniguchi, S.; Okada, T.; Shirakawa, M.; Sakata, Y. *J. Am. Chem. Soc.* **1996**, *118*, 11771. (b) Tashiro, K.; Aida, T.; Zheng, J.-Y.; Kinbara, K.; Saigo, K.; Sakamoto, S.; Yamaguchi, K. *J. Am. Chem. Soc.* **1999**, *121*, 9477. (c) Evans, D. R.; Fackler, N. L. P.; Xie, Z.; Rickard, C. E. F.; Boyd, P. D. W.; Reed, C. A. *J. Am. Chem. Soc.* **1999**, *121*, 8466. (d) Sun, D.; Tham, F. S.; Reed, C. A.; Chaker, L.; Boyd, P. D. W. *J. Am. Chem. Soc.* **2002**, *124*, 6604. (e) Wang, Y.-B.; Lin, Z. *J. Am. Chem. Soc.* **2003**, *125*, 6072. (f) Kimura, M.; Saito, Y.; Ohta, K.; Hanabusa, K.; Shirai, H.; Kabayashi, N. *J. Am. Chem. Soc.* **2002**, *124*, 5274.

(40) (a) Imahori, H.; Guldi, D. M.; Yoshida, Y.; Luo, C.; Sakata, Y.; Fukuzumi, S. *J. Am. Chem. Soc.* **2001**, *123*, 6617. (b) Fukuzumi, S.; Ohkubo, K.; Imahori, H.; Shao, J.; Ou, Z.; Zheng, G.; Chen, Y.; Pandey, R. K.; Fujitsuka, M.; Ito, O.; Kadish, K. M. *J. Am. Chem. Soc.* **2001**, *123*, 10676. (c) Ohkubo, K.; Imahori, H.; Shao, J.; Ou, Z.; Kadish, K. M.; Chen, Y.; Zheng, G.; Pandey, R. K.; Fujitsuka, M.; Ito, O.; Fukuzumi, S. *J. Phys. Chem. A* **2002**, *106*, 10991. (d) Kashiwagi, Y.; Ohkubo, K.; McDonald, J. A.; Blake, I. M.; Crossley, M. J.; Araki, Y.; Ito, O.; Imahori, H.; Fukuzumi, S. *Org. Lett.* **2003**, *5*, 2719. (e) Guldi, D. M.; Imahori, H.; Tamaki, K.; Kashiwagi, Y.; Yamada, H.; Sakata, Y.; Fukuzumi, S. *J. Phys. Chem. B* **2004**, *108*, 541. (f) Ohkubo, K.; Shao, J.; Ou, Z.; Kadish, K. M.; Li, G.; Pandey, R. K.; Fujitsuka, M.; Ito, O.; Imahori, H.; Fukuzumi, S. *Angew. Chem., Int. Ed.* **2004**, *43*, 853.

(41) Hasobe, T.; Kashiwagi, Y.; Absalom, M.; Hosomizu, K.; Crossley, M. J.; Imahori, H.; Kamat, P. V.; Fukuzumi, S. *Adv. Mater.* **2004**, *16*, in press.

(42) (a) Kamat, P. V.; Barazzouk, S.; Hotchandani, S.; Thomas, K. G. *Chem.—Eur. J.* **2000**, *6*, 3914. (b) Kamat, P. V.; Barazzouk, S.; Thomas, K. G.; Hotchandani, S. *J. Phys. Chem. B* **2000**, *104*, 4014. (c) Suddep, P. K.; Ipe, B. I.; Thomas, K. G.; George, M. V.; Barazzouk, S.; Hotchandani, S.; Kamat, P. V. *Nano Lett.* **2002**, *2*, 29.

(43) (a) Imahori, H.; Hasobe, T.; Yamada, H.; Kamat, P. V.; Barazzouk, S.; Fujitsuka, M.; Ito, O.; Fukuzumi, S. *Chem. Lett.* **2001**, 784. (b) Hasobe, T.; Imahori, H.; Fukuzumi, S.; Kamat, P. V. *J. Mater. Chem.* **2003**, *13*, 2515. (c) Hasobe, T.; Imahori, H.; Fukuzumi, S.; Kamat, P. V. *J. Phys. Chem. B* **2003**, *107*, 12105.

(44) (a) Fujihira, M. *Mol. Cryst. Liq. Cryst.* **1990**, *183*, 59. (b) Morita, T.; Kimura, S.; Imanishi, Y. *J. Am. Chem. Soc.* **1999**, *121*, 581. (c) Hirayama, D.; Takimiya, K.; Aso, Y.; Otsubo, T.; Hasobe, T.; Yamada, H.; Imahori, H.; Fukuzumi, S.; Sakata, Y. *J. Am. Chem. Soc.* **2002**, *124*, 532. (d) Lahav, M.; Gabriel, T.; Shipway, A. N.; Willner, I. *J. Am. Chem. Soc.* **1999**, *121*, 258.

(45) (a) Seta, P.; Bienvenue, E.; Moore, A. L.; Mathis, P.; Bensasson, R. V.; Liddell, P. A.; Pessiki, P. J.; Joy, A.; Moore, T. A.; Gust, D. *Nature* **1985**, *316*, 653. (b) Steinberg-Yfrach, G.; Liddell, P. A.; Hung, S.-C.; Moore, A. L.; Gust, D.; Moore, T. A. *Nature* **1997**, *385*, 239. (c) Steinberg-Yfrach, G.; Rigaud, J.-L.; Durantini, E. N.; Moore, A. L.; Gust, D.; Moore, T. A. *Nature* **1998**, *392*, 479.

(46) (a) Shipway, A. N.; Katz, E.; Willner, I. *ChemPhysChem* **2000**, *1*, 18. (b) Kamat, P. V. *J. Phys. Chem. B* **2002**, *106*, 7729.

(47) (a) Brust, M.; Walker, M.; Bethell, D.; Schiffrin, D. J.; Whyman, R. *J. Chem. Soc., Chem. Commun.* **1994**, 801. (b) Templeton, A. C.; Wuelfing, W. P.; Murray, R. W. *Acc. Chem. Res.* **2000**, *33*, 27.

(48) (a) Schmid, G. *Clusters and Colloids: From Theory to Applications*; VCH: New York, 1994. (b) Alivisatos, A. P. *Science* **1996**, *271*, 933. (c) Henglein, A. *Ber. Bunsen-Ges. Phys. Chem.* **1995**, *99*, 903. (d) Pileni, M. P. *New J. Chem.* **1998**, 693. (e) Link, S.; El-Sayed, M. A. *J. Phys. Chem. B* **1999**, *103*, 4212.

(49) (a) Imahori, H.; Kashiwagi, Y.; Hanada, T.; Endo, Y.; Nishimura, Y.; Yamazaki, I.; Fukuzumi, S. *J. Mater. Chem.* **2003**, *13*, 2890. (b) Imahori, H.; Kashiwagi, Y.; Endo, Y.; Hanada, T.; Nishimura, Y.; Yamazaki, I.; Araki, Y.; Ito, O.; Fukuzumi, S. *Langmuir* **2004**, *20*, 73.

(50) Fukuzumi, S.; Endo, Y.; Kashiwagi, Y.; Araki, Y.;Ito, O.; Imahori, H. *J. Phys. Chem. B* **2003**, *107*, 11979.

(51) Hasobe, T.; Imahori, H.; Fukuzumi, S.; Kamat, P. V. *J. Am. Chem. Soc.* **2003**, *125*, 14962.

(52) Ahmadi, T. S.; Logunov, S. L.; El-Sayed, M. A. *J. Phys. Chem.* **1996**, *100*, 8053.

(53) (a) Brun, A. M.; Harriman, A. *J. Am. Chem. Soc.* **1994**, *116*, 10383. (b) Oevering, H.; Verhoeven, J. W.; Paddon-Row, M. N.; Cotsaris, E.; Hush, N. S. *Chem. Phys. Lett.* **1988**, *143*, 488. (c) Schlicke, B.; Belser, P.; De Cola, L.; Sabbioni, E.; Balzani, V. *J. Am. Chem. Soc.* **1999**, *121*, 4207. (d) Barigelletti, F.; Flamigni, L.; Guardigli, M.; Juris, A.; Beley, M.; Chadorowsky-Kimmes, S.; Collin, J.-P. Sauvage, J.-P. *Inorg. Chem.* **1996**, *35*, 136. (e) Closs, G. L.; Piotrowiak, P.; MacInnis, J. M.; Fleming, G. R. *J. Am. Chem. Soc.* **1988**, *110*, 2652.